IS-T--1460

DE91 000663

An Investigation of the Mechanisms of Calcination and Sulfation in Coal-water Mixtures

by

Christofides, Nearchos

MS Thesis submitted to Iowa State University

Ames Laboratory, U.S. DOE

Iowa State University

Ames, Iowa 50011

Date Transmitted: September 21, 1990

PREPARED FOR THE U.S. DEPARTMENT OF ENERGY

UNDER CONTRACT NO. W-7405-Eng-82.

TABLE OF CONTENTS

LIST OF TABLES

LIST OF FIGURES

ACKNOWLEDGMENTS

My special thanks to Professor Robert Brown for his advice and guidance during the progress of my research. I would also like to thank Dr. Jon Van Gerpen and Dr. Thomas Wheelock for serving on my graduate committee program. I also wish to express my sincere thanks to Dr. Jim Foley for his advice and Mr. Rod Othaout for his assistance in preparing the fuel and performing the experiments.

I gratefully acknowledge the Iowa State Mining and Mineral Resources Research Institute and the Ames Laboratory of the United States Department of Energy for their financial support. This work was performed at Ames Laboratory under contract No. DE-FG22-87PC79915 with the U. S. Department of Energy.

1. INTRODUCTION

Coal-water mixtures (CWM) are investigated as fuel in fluidized bed combustors. There are distinct advantages in using CWM in certain applications of FBC. Fuel preparation and handling costs are substantially reduced because the fuel is in liquid form. This advantage may be significant to small-scale and in pressurized FBC (PFBC) applications[1]. Coal-water mixtures were originally formulated for use in oil-fired furnaces[2]. Due to the rheological requirements of spray nozzles, these mixtures require fine coal grinds and addition of dispersants. Of particular interest to FBC are CWM prepared from coarse coal grinds. A number of researchers have demonstrated that these less expensive preparations burn satisfactorily in fluidized beds[1],[2]. Many researchers have observed higher combustion efficiency for CWM compared to dry coal, which has been attributed to the formation of either large agglomerates[3],[4] or small flecks of char attached to sand particles[2] when CWM is sprayed in the bed.

Sulfur removal is also of special interest when CWM are burned in FBC. Previous research on the subject suggests improvements in sorbent utilization when limestone is mixed with CWM[3]. Several other researchers contradict this view by suggesting that sorbent utilization in CWM is degraded by the reaction of calcium sulfate with coal-ash[4]. Roberts et al.[1] showed that CWM and dry coal have comparable

sorbent utilization when fired in PFBC at conventional FBC temperatures. All previous comparisons of sorbent utilization between dry coal and CWM were not made under comparable experimental conditions, that is coal and limestone feedstocks, or combustion conditions were different.

The purpose of this investigation is to study the mechanisms of sulfur capture when burning coal-water-limestone mixtures (CWLM) in fluidized beds. Special care is taken to make comparisons with to dry coal and sorbent under comparable experimental conditions. A series of experiments were performed in an eight-inch diameter bubbling fluidized bed combustor to address this problem.

2. BACKROUND

2.1 The Mechanisms of Combustion of CWM in FBC

A number of researchers have investigated the mechanisms of combustion of CWM in FBC[2],[3],[4],[5]. The mechanisms of combustion of CWM in FBC were also studied by Gregory and Brown [6] and Brown and Christofides[7]. They demonstrated that CWM burn primarily as large char-sand agglomerates formed when the fuel is sprayed in FBC. The agglomeration of the CWM droplets has been studied by a number of researchers, some of whom developed models that explain this phenomenon. De Michelle et al. [8] suggested that the agglomeration occurs in three stages: heating of the droplets that commences as soon as they enter the bed, an evaporation-devolatilization phase during which the volatiles condense on the wet coal surfaces, and a final ash loss phase (Figure 2.1). The final form of the fuel is a porous carbonaceous agglomerate that has sand particles imbedded in its matrix. Arena et al.[2], on the other hand, theorized that CWM burn as char-flecked sand particles formed when individual char particles adhere to bed sand.

Gregory and Brown[6] estimated the average residence time of these agglomerates, in a 6-inch deep sand-bed to be on the order of one minute. They further demonstrated that improvements in combustion efficiency for CWM compared to dry coal burned in FBC are primarily due to the differences in particle sizes between the

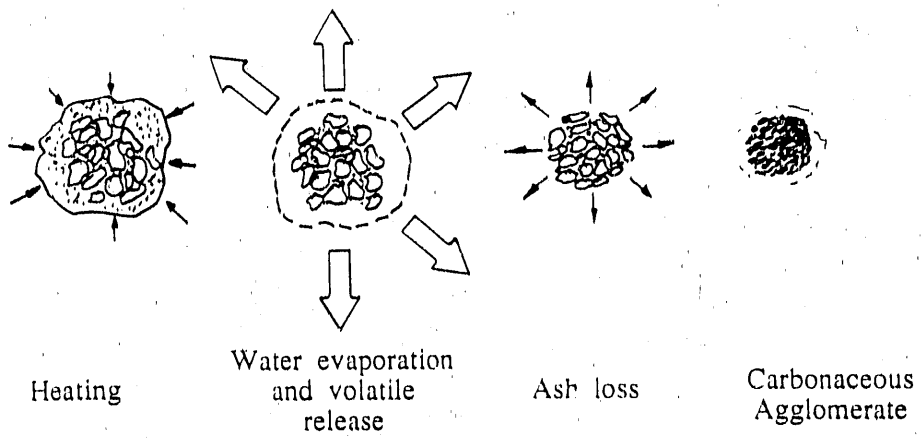

Figure 2.1: De Michelle's model of CWM agglomeration in FBC

two fuels. Attrition of the fuel particles in the bed was found to be of inferior importance. Fragmentation was, instead, shown to be the primary parameter affecting combustion efficiency.

Fragmentation can be explained by the concept of critical porosity obtained from the percolation theory[9]. As coal particles burn, oxygen penetrates the pores and consumes carbon inside the particle, resulting in increased char porosity. When critical porosity is reached, the char matrix collapses producing smaller fragments that are denser than the parent char. Large initial particles will produce large non-elutriable fragments, which will require further percolation to be elutriated.

If a sulfur sorbent is added directly to CWM, then it is expected to enter the bed imbedded in the agglomerates. Consequently, fragmentation is expected to reduce

the sorbent concentration after a finite time.

2.2 Sulfur Release from Coal and the Reaction of SO_2 with Limestone

2.2.1 The mechanisms of sulfur release from coal

Coal contains sulfur in the form of pyrites (e.g., $FeSx$) and as organic sulfur[10]. The mechanism of sulfur release during coal combustion can be described as a two step phase[11]. Most of the sulfur is released during devolatilization. Moffat[11] suggests that the sulfur released during devolatilization is the product of the reduction of organic sulfur compounds and some pyrites by hydrogen. The hydrogen sulfide (H_2S) produced is immediately oxidized to yield water and SO_2. Some additional sulfur is released at the end of the char burnout via oxidation of inorganic sulfides.

2.2.2 Calcination and sulfation of limestone

Calcium carbonate, in the form of limestone and dolomites, is the economically most feasible sulfur sorbent used in fluidized beds. Above 1000 ^oF, $CaCO_3$ undergoes calcination according to the reaction :

$$CaCO_3 \rightleftharpoons CaO + CO_2 \tag{2.1}$$

The resulting CaO matrix is extremely porous and susceptible to reaction with sulfur dioxide (SO_2). The production of pores in the lime structure is essential to sulfur sorption. The porosity of the calcined limestone is a measure of how well it will absorb the SO_2. As calcination commences, the limestone density is substantially reduced.

In the presence of oxygen, sulfur dioxide will react readily with CaO to produce $CaSO_4$ (gypsum). Several researchers[12] suggest that the sulfation reaction follow a two body mechanism, i.e., SO_2 and oxygen will diffuse in the lime pores and adsorb on the lime surface. The surface action occurs in two steps:

$$SO_2 + 1/2O_2 \rightarrow SO_3 \tag{2.2}$$

$$CaO + SO_3 \rightarrow CaSO_4 \tag{2.3}$$

On the other hand, Yates[13] suggests that SO_3 is produced only if heavy metal salts are present to catalyze the reaction of SO_2 with oxygen. Otherwise CaO is first converted to $CaSO_3$ which will oxidize to gypsum.

$$CaO + SO_2 \rightarrow CaSO_3 \tag{2.4}$$

$$CaSO_3 + 1/2O_2 \rightarrow CaSO_4 \tag{2.5}$$

2.2.3 Temperature dependence of sulfur sorption

Sulfur sorption by limestone is temperature dependent. The temperature for maximum sulfur removal lies between 1500 and 1550^oF[10],[14]. The limestone reactivity is dependent on the degree of sulfation. As the degree of sulfation of limestone increases, this peak becomes more pronounced and occurs at lower temperatures[10].

Saxena[15] suggests that at lower than the optimum temperatures, it is possible that sulfation follows an alternative route as expressed by the reaction:

$$CaCO_3 + SO_2 + O_2 \rightarrow CaSO_4 + CO_2 \tag{2.6}$$

This reaction tends to reduce the rate of sulfation.

2.2.4 Limestone decomposition and pore plugging

At temperatures above the optimum there may be a variety of events that reduce sulfation rates. Several researchers[4],[11] suggest that $CaSO_4$ will either decompose to CaO and SO_2, or it will react with coal ash to form silicates with the release of SO_2.

$$\begin{aligned} CcSO_4 &\rightarrow CaO + SO_2 + 1/2O_2 \\ CaSO_4 + ash &\rightarrow silicates + SO_2 + 1/2O_2 \end{aligned} \tag{2.7}$$

Sorbent utilization may also be reduced by inhibition of the sorbent due to closure of the pores in the lime matrix. Pore plugging is one of the main problems anticipated when limestone is used as a sulfur sorbent. Due to its large molar volume $CaSO_4$ will build up in the lime pores and reduce the rate of diffusion of SO_2, thus reducing the rate of sulfation.

Simons et al.[16] modelled lime pores as similar to tree branches. The big and small branches of a tree describe the progression of pores from larger to smaller size. If the deposition of gypsum begins in the small pores and slowly progresses to the outer surface, then the utilization of the effective sorption area is increased. On the other hand, if sulfation rate is fast enough, then the larger pores become filled with gypsum, thereby controlling the rate of diffusion of SO_2 to the inner surface of the lime.

2.2.5 The effect of substoichiometric conditions on sulfation

It has been observed that under reducing conditions sulfur will not oxidize, but instead reduce to hydrogen sulfide (H_2S). Hydrogen sulfide in turn will react with

lime forming calcium sulfide (CaS)[11],[14]:

$$CaCO_3 + H_2S \rightarrow CaS + H_2O + CO_2 \quad (2.8)$$

$$CaO + H_2S \rightarrow CaS + H_2O \quad (2.9)$$

Calcium sulfide has substantially lower molar volume than gypsum, therefore severe pore plugging is prevented. Jonke et al.[14] observed that CaS is the main product of sulfation when the oxygen concentration in the bed is reduced to around 50% of the stoichoimetric amount. The sulfide production is reduced to 2% when the bed oxygen concentration is increased to above 70 to 80%. Once exposed to the atmosphere, CaS will readily oxidize to $CaSO_4$.

2.2.6 Factors that improve sorbent utilization

The use of a fine sorbent grind has been observed to improve sulfur sorption. Theoretically there is a minimum particle size of 6 microns for which the sorbent utilization approaches unity (see Figure 2.2)[17]. In practice, the minimum particle size is limited by the superficial velocities used in the fluidized bed. Bonn and Münzner[17] have estimated this minimum to be of the order of 380 microns. The minimum size may further be increased for calcined limestone, since the release of CO_2 during calcination reduces the density of the sorbent.

Green[18] has observed that sorbent utilization may be improved by incorporating abrasives in the bed. They reasoned that the abrasives grind the crust of $CaSO_4$ formed on the outer surface of the sorbent particles, thus recovering fresh active sites.

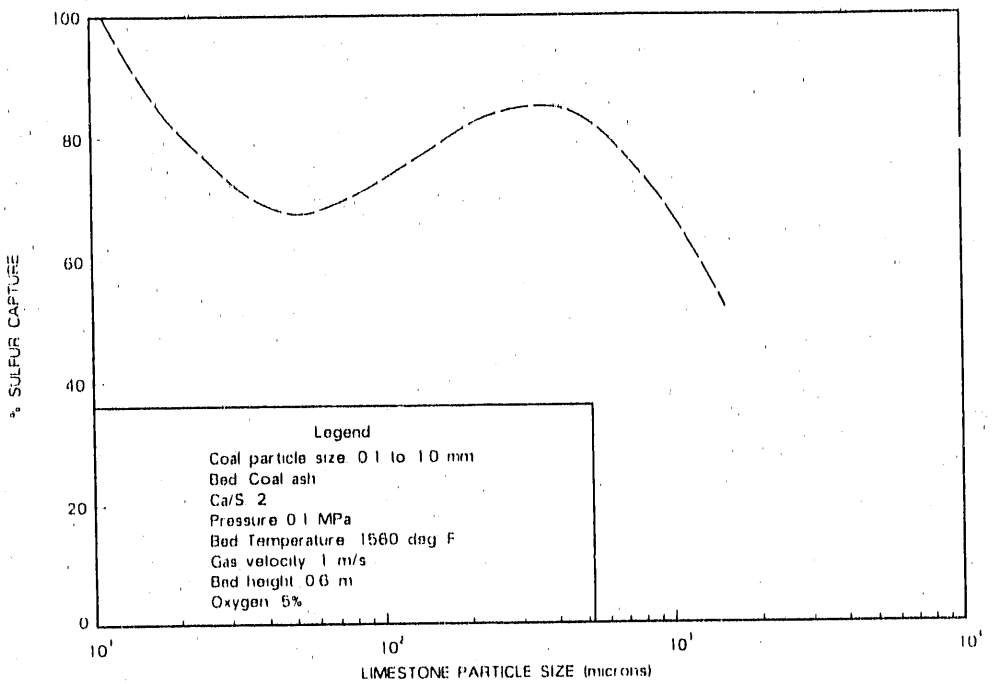

Figure 2.2: Particle dependence of SO_2 capture

2.2.7 Limestone regeneration and hydration

It is well known that limestone may be recycled after being regenerated by reductive decomposition [10]. Reductive decomposition involves the reaction of $CaSO_4$ with either CO or H_2 at temperatures in the range 1830 to 2010 ^oF:

$$CaSO_4 + CO \quad \rightarrow \quad CaO + SO_2 + CO_2 \tag{2.10}$$

$$CaSO_4 + H_2 \quad \rightarrow \quad CaO + SO_2 + H_2O \tag{2.11}$$

The treatment gas, which is a mixture of H_2 and CO, may be produced from the combustion of coal under slightly substoichiometric conditions. A small progressive loss of reactivity occurs with each regeneration cycle, mainly because of incomplete regeneration.

A less expensive process to partially recover unreacted lime from limestone par-

ticles is hydration. The unreacted sorbent particles enter the FBC where they react with SO_2 forming a dense layer of $CaSO_4$ around a core of residual CaO. Partial hydration of the semi-reacted sorbent generates $Ca(OH)_2$, the molar volume of which is much larger than that of CaO. The expansion of the core of the treated particles produces cracks in the surface layer of $CaSO_4$. The partially hydrated sorbent is re-introduced to the bed where it is subjected to simultaneous dehydration and sulfation. These processes take place in the core of the particles. The hydration of the sorbent may be repeated until the entire matrix of CaO is converted to gypsum[5].

2.3 Sulfur Capture When Burning CWM

Cen et al.[3] were among the first to directly introduce limestone to CWM. They suggested that the intimate contact of limestone and coal in the char-sand agglomerates would improve sulfur capture. On the other hand, Mei et al.[4] pointed out that limestone incorporated into the agglomerates will calcine and sulfate at temperatures typical of char combustion, which may be as much as 300 ^oF higher than the bed[19]. These temperatures may be higher than the desired optimum for sulfur sorption. Decomposition of $CaSO_4$ in the agglomerates, at these higher temperatures, will reduce sorbent utilization. Limited experimental evidence supports the hypothesis that incorporation of limestone in CWM will improve sorbent utilization[3],[20].

Sulfation within the agglomerates has not yet been demonstrated experimentally. Trivett et al.[20] implied that the mechanism of sulfur sorption involves the capture of SO_2 by free floating CaO particles in the bed. These particles are supposedly released after the agglomerates break. Brown et al.[5] tested Trivett et al.'s[20] hypothesis by injecting coal-water-limestone mixtures (CWLM) in sand beds of different depth.

They determined that SO_2 sorption increased with bed depth, suggesting that Trivett et al.'s[20] hypothesis is correct. If sulfation occurred solely within the agglomerates, then bed depth should have little or no effect on sulfur retention. On the contrary, if sulfation occurs after individual CaO particles are released to the bed upon attrition or fragmentation[20] of agglomerates, then sorbent utilization is expected to increase with increasing bed depth.

Foley et al.[21] compared sorbent utilization for CWLM with results for dry coal in a limestone bed obtained from Stantan[22]. They estimated that the optimum temperature for sulfur sorption when burning CWLM to be as much as 200 ^oF higher than for the dry fuel and sorbent. If the limestone is trapped in the agglomerates, then it is most likely expected to calcine and sulfate at the particle temperatures which are as much as 200 ^oF higher than the bed.[19] Consequently, the optimum temperature for sulfur retention might be lower for coals that incorporate limestone in their ash.[23]

The present experimental evidence, concerning the mechanisms of sulfur removal during combustion of CWLM in FBC, is not sufficient for deriving a definitive conclusion.

3. EXPERIMENTAL APPARATUS

3.1 Combustor

The 8-inch diameter fluidized bed combustor is shown schematically in Figure 3.1. The distributor plate at the bottom of the bed is a stainless steel plate perforated with 250 3/32-inch holes. A 100-mesh stainless steel screen, spot welded on the plate, The main body of the combustor consists of a mild steel cooling water jacket the inner part of which is lined with a 1-inch thick layer of Kaocast RFT castable refractory. The plenum at the bottom of the bed serves as a mixing chamber for the air and Liquified Petroleum (LP) gas mixture during the preheat cycle.

A 4-foot long mild steel freeboard extends above the main body of the combustor. The freeboard serves both as an afterburner for elutriated fines, thus improving combustion efficiency, and as a muffler. The flue gas exits the combustor via a roof-mounted exhaust fan that draws the exhaust from a pipe at the top side of the freeboard.

Two 1-foot long electrodes (not shown) connected to a 10-kvolt transformer provide the ignition spark for initiating the preheat gas flame. The electrodes are bend downwards to ignite the L-P gas as close as possible to the fluidized bed.

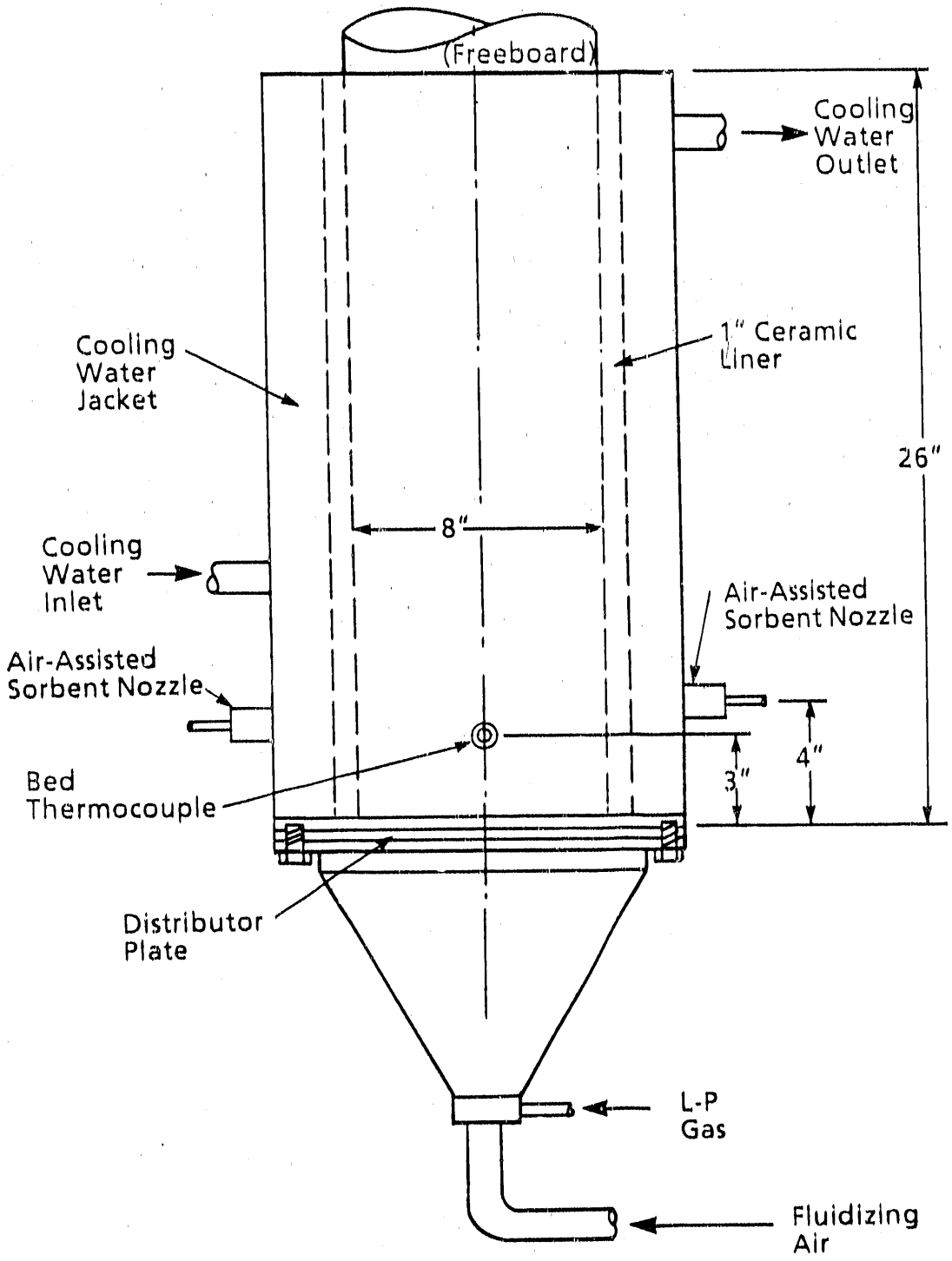

Figure 3.1: The combustor

3.2 Fuel and Sorbent Feeding Systems

A schematic of the experimental apparatus is shown in Figure 3.3. Dry fuel is fed by an Accurate Model 602 dry material feeder via a port at the bottom of the freeboard. The feeder is fitted with a $1\frac{3}{4}$-inch diameter center-screw. The feed rate delivered by the auger is calibrated, for each material fed, versus the motor setting counter.

An air assisted nozzle provides the means for feeding CWM. The fuel is pumped from a small reservoir using a variable speed rotary pump. A bypass line returns a large portion of the flow to the reservoir, leaving a flow in the range of 10-60 lb/hr to fire the combustor.

The CWM nozzle (Figure 3.4) consists of three concnentric tubes. The outer 3/4-inch diameter tube is made of stainless steel. The intermediate black-steel tube is of 1/4-inch I.D.. The annulus between the two outer tubes serves as a water jacket for cooling the nozzle. A third 1/4-inch stainless steel tube provides the inlet for the fuel. Air at 1.5 scfm is passed through the inner annulus to assist the CWM dispersion in the bed. The nozzle is installed 4-inches above the bottom of the bed.

Dry sorbent is fed at the bottom of the bed via another air assisted system (Figure 3.5). A 4-inch diameter plexiglass hopper feeds dry sorbent to a 1/4-inch screw feeder, which is driven by a Dayton Model 2Z803B 1/15 HP variable speed gear motor. The feeder drops the sorbent particles in an air stream via a 1/8-inch venturi. An agitator driven by a small A/C motor is used in the hopper to prevent bridging of the sorbent. A 3-scfm air stream conveys the sorbent to the bottom of the bed via a 3/32-inch water-cooled nozzle. The nozzle is of similar design to the CWM nozzle. The feeder feed rate is calibrated versus the motor input voltage for

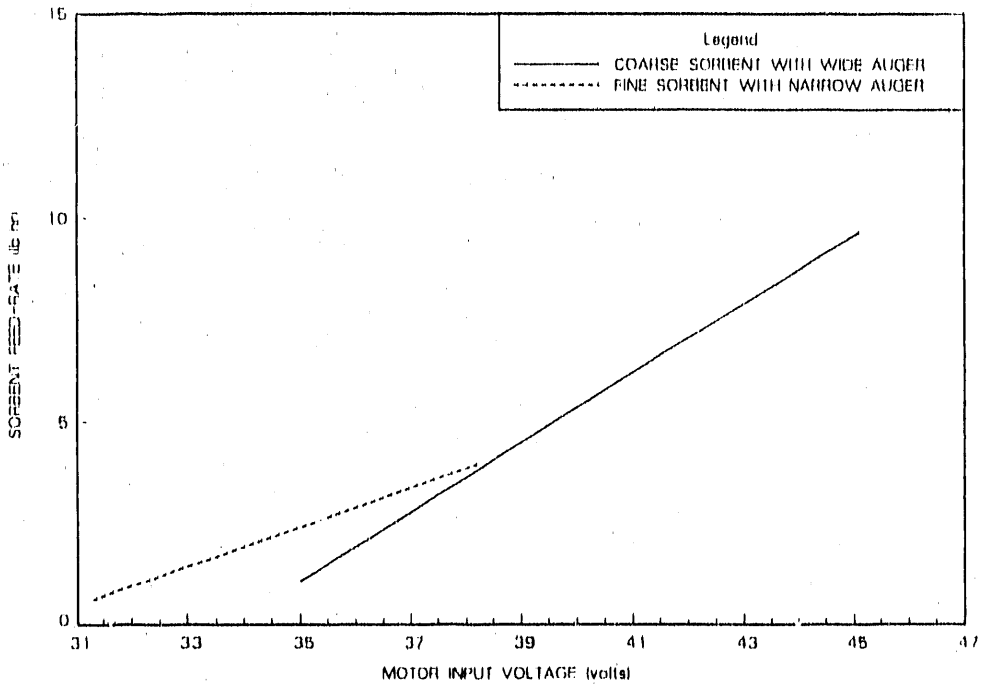

Figure 3.2: Dry limestone feeder calibration

each sorbent size. The calibration lines are shown in Figure 3.2.

3.3 Gas Sampling System

Five gas analyzers are used to monitor flue gas composition: two Beckmann Model 870 nondispersive infrared spectrometers for CO and CO_2 compositon; a Beckmann Model 755 oxygen analzer ; and two Horiba Models VIA-300 and VIA-500 nondispersive infrared spectrometers for NO_x and SO_2.

A sample of flue gas is drawn from the top of the combustor freeboard via a sampling probe, which is pointed away from the flow to reduce the the number of particles entering the sampling tube. Filtering and drying of this gas sample prior to analysis is necessary to protect the instruments and to prevent interference with

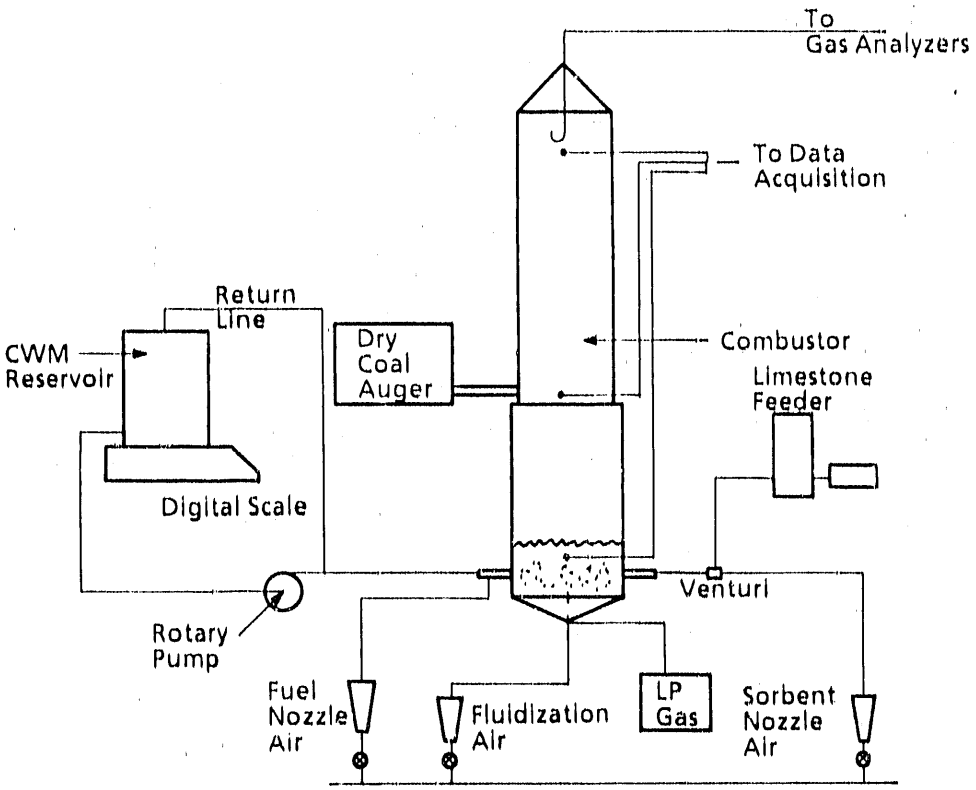

Figure 3.3: Experimental apparatus

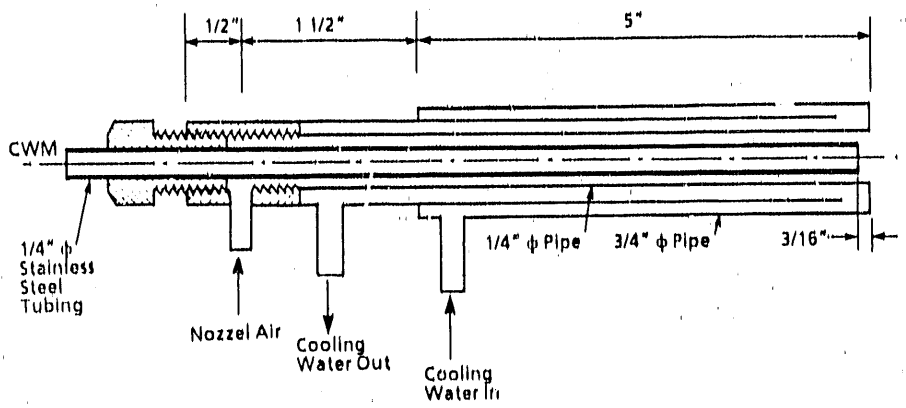

Figure 3.4: CWM nozzle

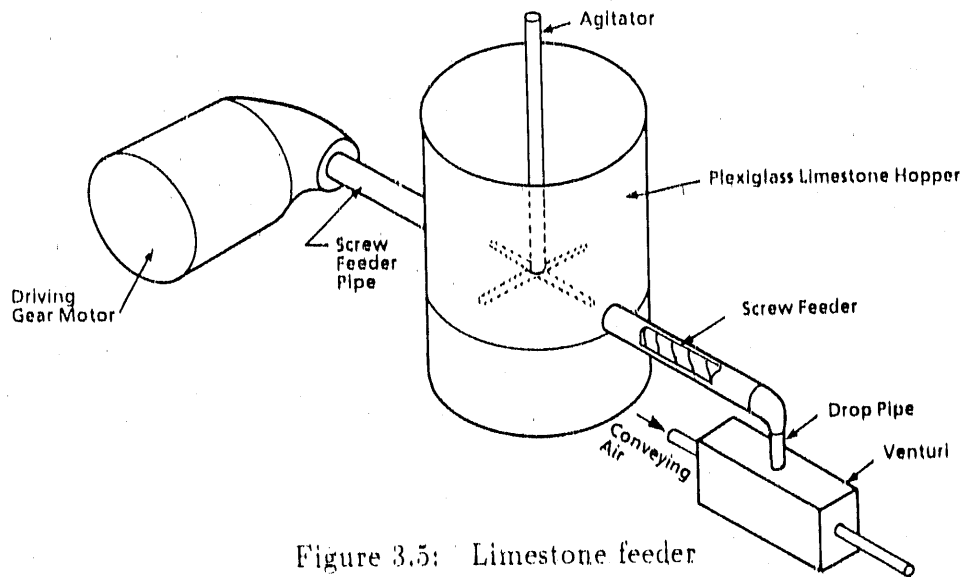

Figure 3.5: Limestone feeder

the readings. This is achieved by first passing the gas through a Balston Type 30/12 particulate filter to collect all solids entrained by the flow, and then through an acid mist filter to collect any tar and acid vapor present in the sample. To prevent condensation prior to drying, all lines are heat traced to 400 ^{o}F. The Balston filter is maintained at 250 ^{o}F, and the acid mist filter at around 200 ^{o}F. A detailed diagram of the sampling system is shown in Figure 3.6.

A Perma-Pure Model PD625-24APS dryer is used to remove moisture from the sample stream. The dryer consists of a bundle of semipermeable membrane tubes. The tube bundle is enclosed in a stainless steel tube. The moist flue gas is passed through the membrane tubes. A dry purge stream of air is passed outside the membranes. In this manner, a partial pressure gradient is generated and the moisture from the flue gas diffuses through the walls of the membrane tubes into the purge stream. The dryer must be maintained at a temperature of 170 ^{o}F for optimum moisture removal. The dry purge stream is generated by a Perma-Pure Model HD202-b heatless dryer which dries the air to a dew point of -50 ^{o}F. Under normal circumstances, the flue gas dryer is capable of drying the flue gas stream to a dew point of 10-15 ^{o}F. However, prolonged operation of the dryer results in the contamination of the membrane walls and reduces the performance of the dryer. Also, the combustion of CWM results in large amounts of moisture in the flue gas. In the event that the dew point of the flue gas gets high enough prior to drying, the moisture will condense and dissolve SO_2, forming sulfuric acid. The latter will eventually adhere on the membrane walls and reduce the performance of the dryer.

To detect any condensate formed in the system and to detect the possible formation of sulfuric acid, an impingement filter is installed after the dryer. Acidity tests

on these samples showed a pH between 2 to 3. The amounts of acid formed were estimated by measuring the volume of the condensate and performing simple acid equilibrium calculations. A representative sample of calculations is carried out in the Appendix. Tests showed that the amount of acid formed is close to $6 \times 10^{-4}\%$ (on a wet gas basis) which is low enough so that the reading is not considerably affected.

3.4 Data Acquisition System

The data acquisition system consists of a Zenith Z-128 microcomputer. Temperatures are measured using chromel/alumel (type K) thermocouples installed at the locations shown in Figure 3.3. A thermocouple probe is used to measure the bed temperature. The thermocouples are connected to two Metrabyte Model EXP-16 sub-multiplexer boards provided with a cold junction compensation. The boards carry an amplifier that boosts the voltages from the thermocouples. An 8-channel type DAS-8 D/A converter converts the analog signal from the reading boards into a digital equivalent fed in the computer. A program written in Quick Basic 4.0 monitors the output of the DAS-8. All data are monitored continuously. The recording period may be entered as desired and may vary from 0.1 seconds to an unspecified top limit.

Main air flow-rates are continuously measured by a Schaevitz Model P3061 linear variable displacement transformer (LVDT) pressure transducer. Due to zero shift on the pressure transducer the reading has to be compensated by correcting for the shift when the flow is off. The analog output from the transducer is fed directly to the DAS-8 which converts it to computer compatible data. Nozzle air flow-rates are monitored and measured manually using two variable-area flow-meters.

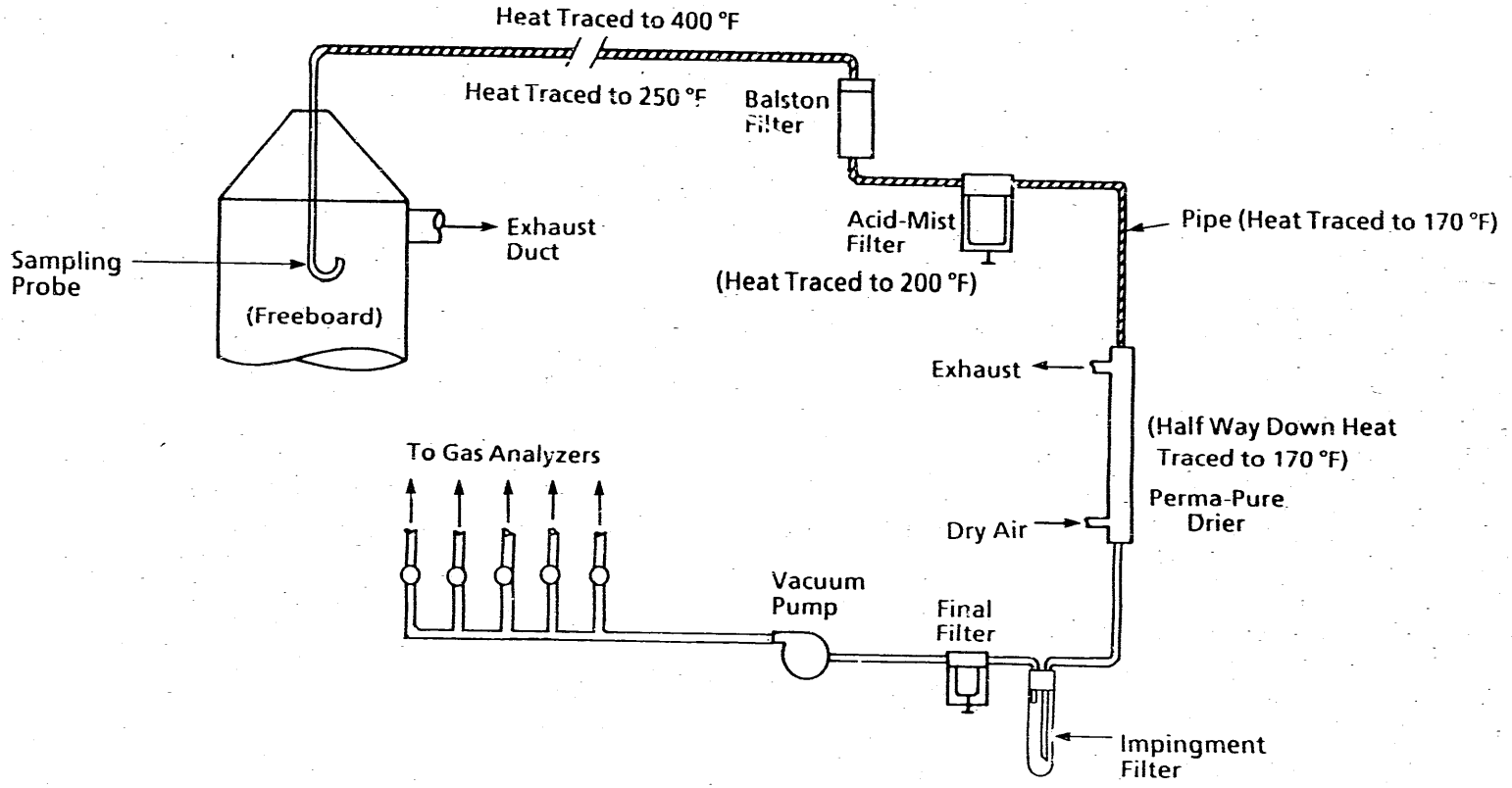

Figure 3.6: Gas sampling system

An Arlyn electronic digital scale is used to measure the CWM flow-rate. The output from the scale is directly fed to the computer routine, which calculates the mass flow rate of the fuel every 1.5 minutes. Visual inspection is also possible since the routine displays continuously the mass of the CWM reservoir.

Flue gas analysis is made possible by directly connecting the outputs from the gas analyzers to the computer via the DAS-8. All data are recorded on either a $5^1/_4$ floppy disc or the 20 megabyte hard disc.

4. MATERIALS AND METHODS

4.1 Fuels and Sorbents

All tests were carried out using Illinois N^o5 seam coal obtained from the Peabody Coal Co., Freeport, Illinois. An analysis of the bituminus coal is given in Table 4.1. The dry fuel was obtained as prepared and had a particle size distribution of 3/8-inch$\times$8-mesh.

CWLM are prepared from the product of a hammermill pulverizer. Dry coal and limestone are crushed separately in the hammermill fitted with a 1/16-inch screen. They are then mixed in proportions, to give a Ca/S ratio of 2. The coal-limestone mixture is blended with water to give a 57% by weight solids loading. No dispersants are used in preparing CWM.

Coal-limestone briquettes are prepared from the same coal-limestone mixture as the CWM. A binder, consisting of 22% corn starch and 78% water, is separately prepared in a blender and added to the coal-limestone mixture. The proportions of coal/limestone/binder are 1/0.164/0.164 respectively. The binder is worked thoroughly in the dry mixture until no lumps are visible. Briquettes are formed in a briquetting machine that compresses the mixture between two form rolls to a pressure of 1400 psi.

Limestone is obtained from the Gilmore City formation in Iowa. An analysis is

Table 4.1: Coal analysis

Proximate Analysis (as received)	
Moisture	10.8%
Ash	10.1%
Volatile Matter	36.0%
Fixed Carbon	42.5%
Btu/lb	11,395
Ultimate Analysis (dry basis)	
Hydrogen	3.76%
Nitrogen	1.49%
Oxygen	2.57%
Sulfur	3.00%
Ash	11.30%
Free-Swelling Index	4

Table 4.2: Analysis of the Gilmore City limestone

Constituent	Amount by weight
SiO_2	2.02 %
Al_2O_3	1.00 %
Fe_2O_3	0.40 %
MgO	1.93 %
CaO	93.36 %
Na_2O	0.18 %
K_2O	0.02 %
TiO_2	0.05 %
MnO	0.01 %
P_2O_5	0.10 %
SO_3	0.94 %

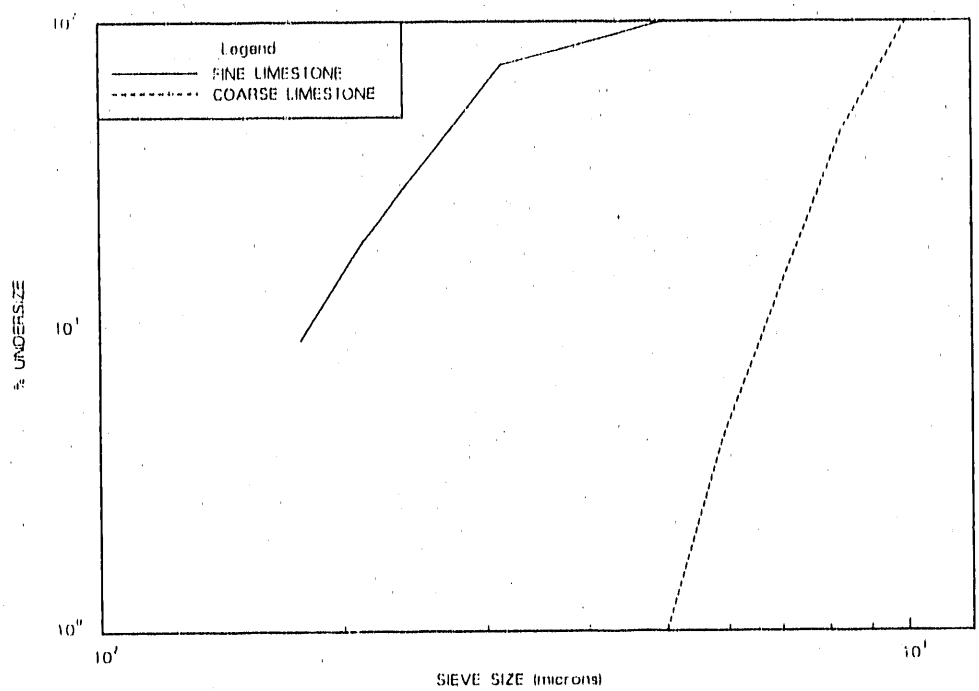

Figure 4.1: Limestone size distribution

given in Table 4.2. Two limestone grinds were used in the experiments: a fine grind (270-mesh × 20-mesh) that was the same as the one used for CWM and briquettes, and a coarser 35-mesh × 18-mesh grind.

The coarse grind was prepared by double screening the product of a roll-mill crusher. A particle size distribution is shown in Figure 4.1.

4.2 Methods and Techniques

Dry coal tests were initiated by preheating the bed with L-P gas until the bed temperature reached 1300 ^{o}F. At this point, the feed rate of dry coal was initiated and the fluidization air was adjusted to compensate for the extra fuel. As soon as the bed temperature increased, the L-P gas was turned off and the air was adjusted

for stoichiometry. A nominal 20% excess air was used for each test. Bed temperature was adjusted by varying the firing rate. When both bed temperature and SO_2 concentration levelled out, the feed rate of sorbent was initiated.

To ensure that a steady state was reached, the data recording routine was initiated as soon as the sorbent feed rate was turned on. At the end of the test, SO_2 concentration was plotted versus time and the steady state was determined.

Coal-water mixture tests were different in the steady state portion. Again the bed was preheated with L-P gas. The fuel flow was initiated at around 1470 ^oF to compensate for the water in the fuel. The air was then adjusted to account for the extra fuel. As soon as the temperature increased, the L-P gas was turned off and the air was adjusted at 20% excess. Combustion of CWM quickly achieved a steady state. A few minutes after the temperature stabilized, the SO_2 concentration in the flue gas reached a steady state.

After approximately four tests, the bed material was screened to prevent build-up of ash. The main reason for the material accumulation was the agglomeration of flyash in the bed.

Nozzle air was adjusted according to test conditions. No air was used through the fuel nozzle during the dry coal tests. A 3-scfm air flow was used to convey the limestone in the bed. During the CWM tests, 1.5-scfm of air were used in the fuel nozzle to enhance spraying. An equal flow rate was used in the sorbent nozzle to ensure equal bed dynamics.

Data were recorded every 4 seconds for all steady state tests, whereas a sampling period of 3 seconds was used for the transient tests. The data were stored in a print-file which could then be imported into Lotus 1-2-3 and processed. The data for

temperature, SO_2, and O_2 concentrations were averaged over the duration of the steady state (typically a period of 20 to 40 minutes).

5. RESULTS AND DISCUSSION

5.1 Investigating the Mechanisms of Calcination and Sulfation of Limestone in CWLM

5.1.1 Comparison of sorbent utilization for CWLM and dry coal

Roberts et al.[1] report no substantial difference in sorbent utilization for CWLM and dry coal during pressurized fluidized bed combustion. On the other hand, several researchers [3],[4],[5],[20],[21] have reported improved sorbent utilization for CWLM compared to dry coal in atmospheric fluidized beds, but failed, in one way or another, to assure comparable experimental conditions for the two fuel forms. To compare sorbent utilization for the two fuel forms, CWLM and dry coal were prepared from the same coal feed-stock. The same finely ground limestone was used as a sorbent for both fuels. Initially two tests were performed at temperatures around $1500 \pm 18^{o}F$. Percent excess air was maintained at a nominal 20%. The calcium to sulfur ratio was 2 : 1 for both tests. The sorbent utilization for the tests is shown in Figure 5.1.

The CWLM test was performed at $1505^{o}F$ and gave a sorbent utilization of 32%. On the other hand, the dry coal and fine sorbent test was carried out at $1518^{o}F$ and resulted in a 20% sorbent utilization, which is substantially lower compared to the CWLM. The fact that the sorbent was very fine raised the suspicion that a fairly

large amount was elutriating from the bed. From basic fluidized bed theory, the diameter of elutriable particles can be estimated from the Equation 5.1:

$$d_{p-spherical} = \sqrt{\frac{18\mu u_t}{(\rho_s - \rho_g)g}} \tag{5.1}$$

It was estimated that limestone particles finer than 175 microns would immediately be entrained by the flow and leave the bed unreacted. Calcination, by reducing particle density, allowed particles as large as 200 microns to quickly elutriate. From Figure 4.1, it was estimated that at least 20% of the limestone was leaving the bed prior to sulfation.

The dry coal test was repeated using the coarser grind of sorbent described above. It was estimated that 99% of this sorbent remained in the bed until attrition acted to reduce particle sizes. The results of this test are also shown in Figure 5.1. The coarser limestone yielded a sorbent utilization of 30% at 1498^oF, which is comparable to the result obtained for fine limestone incorporated in CWM. The results of the above tests are in agreement with the pressurized fluidized bed results presented by Roberts et al.[1]. These tests indicate that CWLM and dry coal have comparable sorbent utilization at conventional FBC temperatures.

5.1.2 Optimum temperature for sulfur retention

The mechanism of sulfur sorption by limestone is strongly dependent on temperature. The optimum bed temperature at which the sulfur sorption efficiency is maximum lies between 1510 and 1550 ^oF[19].

Basu[19] has shown that coal particles burn at temperatures as much as 360^oF higher than the bed, depending on particle diameter. Furthermore, if the limestone which is incorporated in the CWM calcines and sulfates within the agglomerate, it is

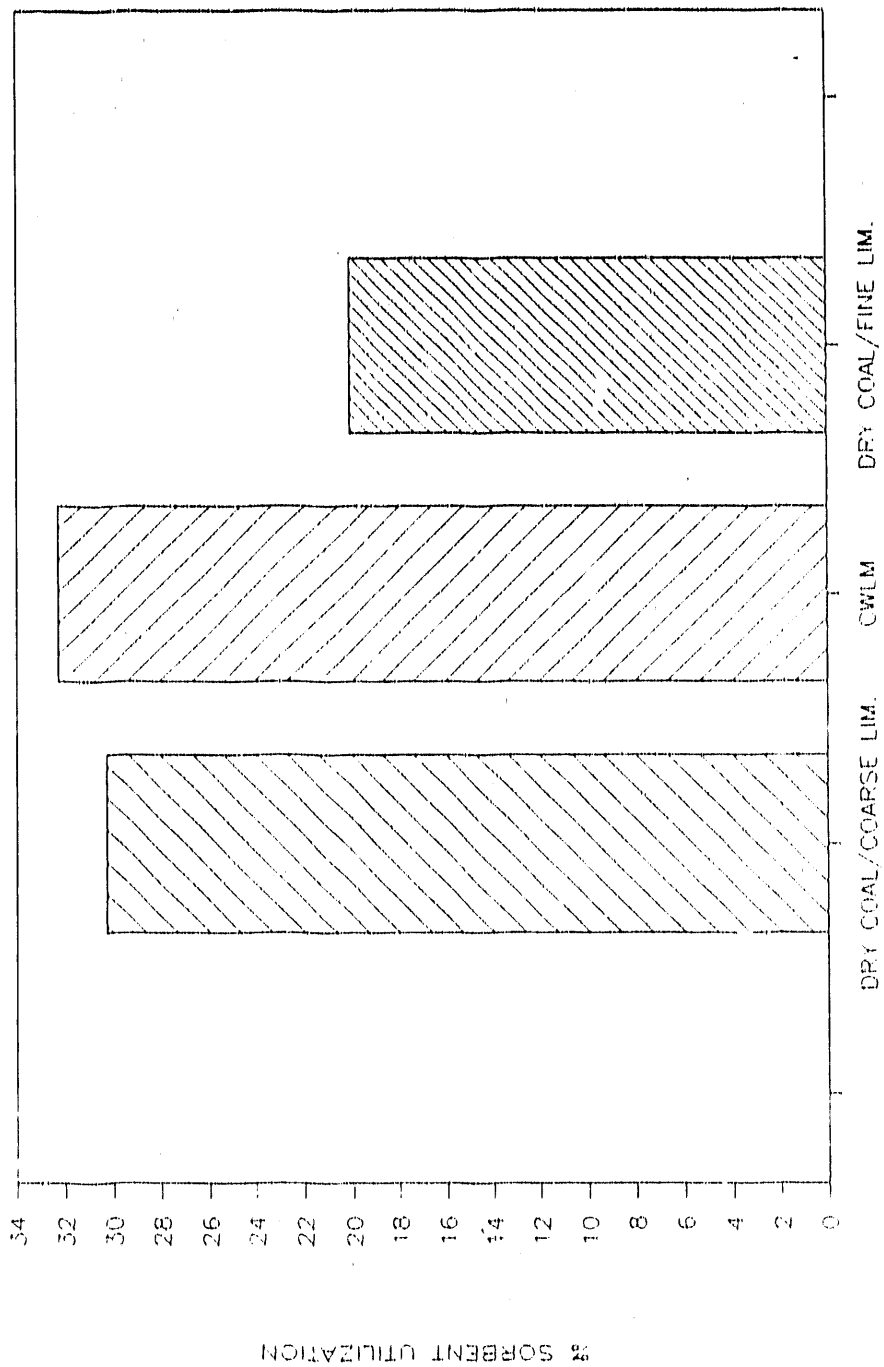

Figure 5.1: Sorbent utilization for CWLM and dry coal

expected to follow closely the temperature history of the agglomerate. Mei et al. [4] were the first to suggest that sorbent utilization may be degraded if limestone is added directly to CWLM. They reasoned that $CaSO_4$ will react with coal ash, at the higher particle temperatures, and decompose. In such case, the optimum temperature for desulfurization when burning CWLM should be expected to be lower than for dry coal. This hypothesis was tested by repeating the tests in Section 5.1 over a range of temperatures. The temperature was varied by changing the firing rate in the combustor. Percent excess air was maintained at 20%.

The percent sulfur sorption as a function of temperature for CWLM and dry coal with fine limestone is shown in Figure 5.2. Sulfur retention for CWLM reaches a maximum of 77% at around 1460^oF. There is no distinct maximum for the dry fuel, but the data suggest that the maximum occurs well above 1520^oF. Furthermore, the largest sulfur retention for CWLM was significantly higher then the respective maximum for dry coal and sorbent. The peculiar behavior of the dry coal/fine sorbent curve may be attributed to increased sorbent elutriation with increasing firing rate in the combustor. Several additional tests were performed, this time with the coarser sorbent. The results are compared to CWLM in Figure 5.3. The peak sulfur sorption for the coarser sorbent occurs around 1520^oF and is approximately 62%, which is much lower than the CWLM peak.

The CWLM peak is 50-60^oF lower than optimum temperature for dry sorbent, which is in qualitative aggreement with Foley et al. [21] who observed peaks for CWLM at temperatures about 200^oF lower than for dry coal (the typical agglomerates were larger for Foley et al.[21] since they were feeding CWLM above the bed). The fact that the peak sorption for CWLM occurs at a lower temperature than for

dry coal suggests that both calcination and sulfation occur in the agglomerates.

5.1.3 Further confirmation that calcination and sulfation occur in the agglomerates

To confirm that calcination and sulfation occur in the char-sand agglomerates, bed material was recovered from the bed after quenching the bed with nitrogen gas. After preheating the bed, CWLM is fed until steady state is achieved. The steady state is maintained for a certain period of time and then the fuel and air are shut off simultaneously, while nitrogen gas is introduced in the bed to quench the combustion. The flow of nitrogen is continued until the bed has cooled sufficiently to stop all reactions. The bed material is then recovered and the agglomerates are separated by screening.

Agglomerated material was recovered from the bed and ground to a fine particle size in a Spex shatterbox. The sample was then subjected to elemental analysis via X-ray fluorescence. The total sulfur in the sample was estimated to be 3-5% by weight. It is obvious that, since the sulfur content of the coal is close to 3%, much of the sulfur is being retained in the agglomerate.

As mentioned in Section 2.2.1, most of the sulfur is expected to be released from the coal upon devolatilization. Very little sulfur is retained in the char of which the agglomerate is composed. To confirm the rapid sulfur release from the Illinois N^o5 seam coal in use, a transient test was performed with 3/8-in$\times$8-mesh dry coal burned in a sand bed with no sorbent addition. Upon reaching steady state, the fuel was shut off and the fluidizing air was slightly reduced to increase the residence time of the coal particles in the bed. The decay in SO_2 emissions, as sulfur was released

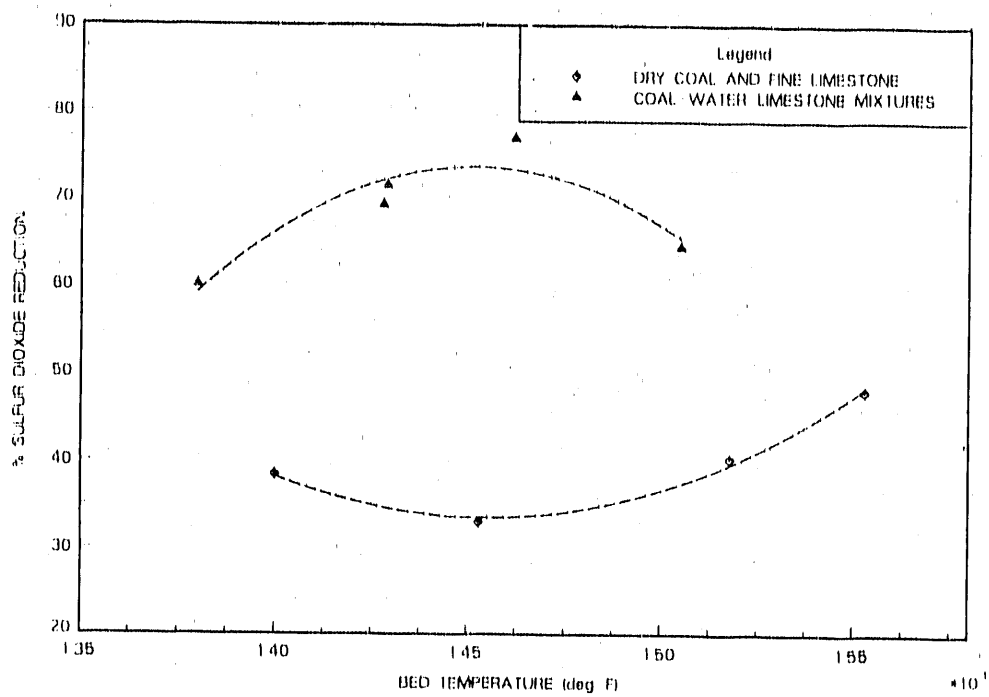

Figure 5.2: Percent sulfur reduction vs. bed temperature for fine limestone and CWLM

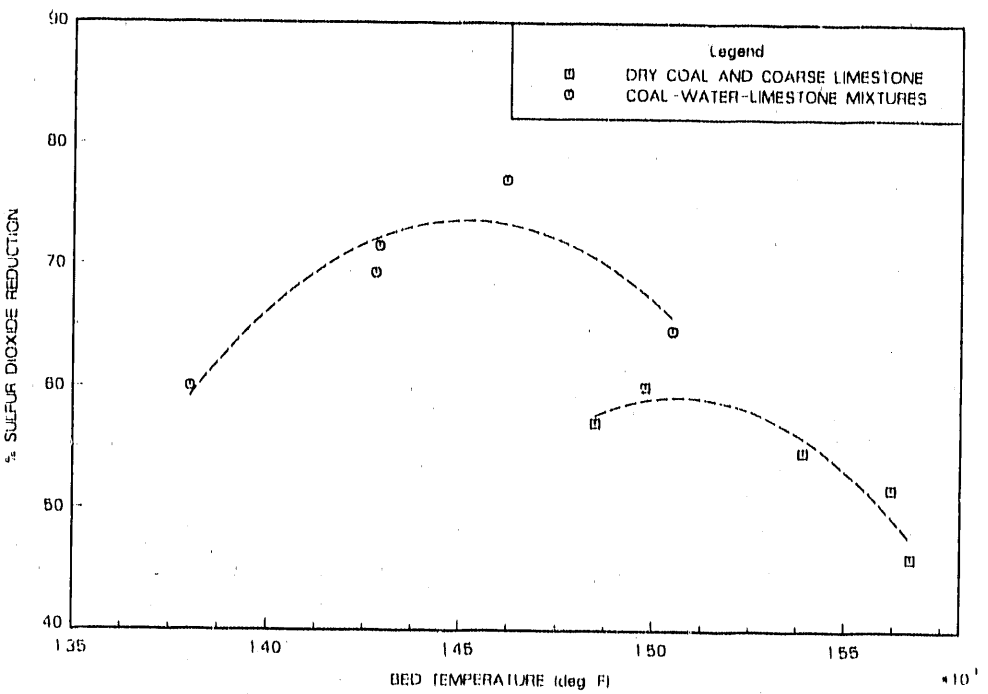

Figure 5.3: Percent sulfur retention vs. bed temperature for coarse limestone and CWLM

from the coal remaining in the bed, was recorded every 3 seconds. A plot of the first two minutes of the transient test is shown in Figure 5.4. This rapid volatile release is followed by a more gradual decline as the small amount of sulfur remaining in the char is being oxidized.

5.1.4 The effect of reducing conditions in the agglomerate

The tests described in the previous section show distinct differences in the sulfur sorption mechanisms of CWLM and dry coal. It is clear that CWLM have improved sorbent utilization compared to dry coal at their respective peaks. Also this peak for CWLM occurs at a much lower temperature than for dry coal. These differences may be attributed to a variety of reasons.

Saxena[15] suggested that under reducing conditions, the sulfation mechanism may become more efficient due to the formation of CaS instead of $CaSO_4$. The former compound has a much smaller molar volume than $CaSO_4$, thereby preventing plugging of the sorbent pores and improving sulfur capture. It is possible that reducing conditions may exist in the vicinity of the agglomerate[24].

To test this hypothesis, a second sample of the agglomerates, recovered from the quench test described above, was finely ground and subjected to X-ray diffraction (XRD) scan. The readings from the XRD scan are shown in Table 5.1. The test showed the presence of $CaCO_3$, anhydrated $CaSO_4$, and CaO. The total amount of calcium compounds is approximately three times that of calcium sulfate. Only small amounts of CaO were detected. These results suggest about 30% sorbent utilization. No other sulfur compounds were detected in the sample.

The quench test was performed at 1380 ^oF where the sorbent utilization is

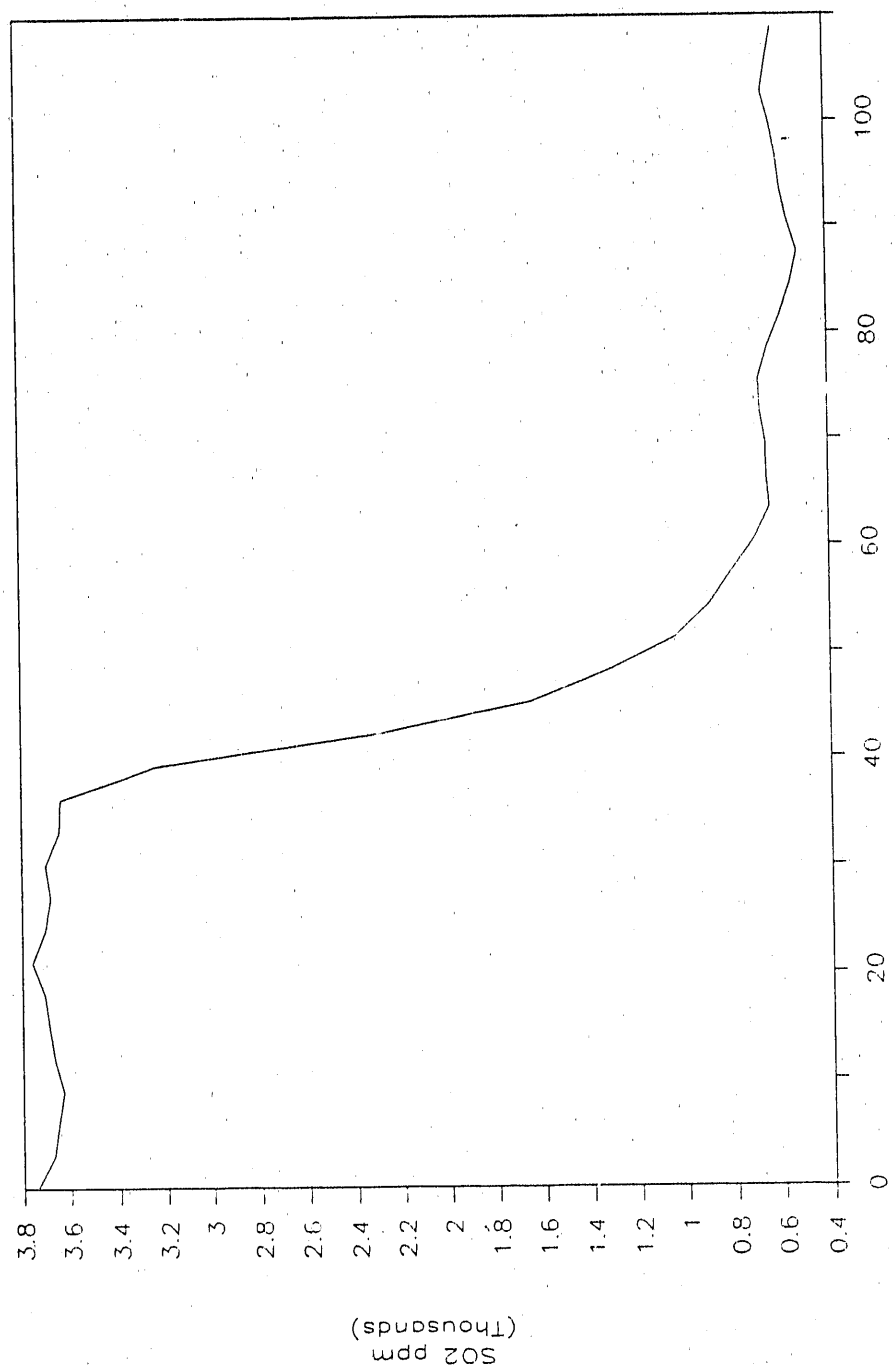

Figure 5.4: Decay in the SO_2 emissions during dry coal transient test

Table 5.1: Results of the X-Ray Diffraction scan on the agglomerates

Mineral's Name	Cemical Formula	Counts
Calcite	$CaCO_3$	150
Quartz, low	SiO_2	150
Anhydrite	$CaSO_4$	70
Feldspar, undefined	$(Na, K, Ca)(Si, Al)_4O_8$	—

predicted to be around 30% (on a molar basis) for the CWLM in use. The results of the XRD scan suggest that the improved sorption for the CWLM at the lower temperatures is not due to reducing conditions in the agglomerate.

Furthermore, the fact that only small amounts of CaO were detected suggests relatively fast sulfation of the sorbent. As soon as the lime calcines, it reacts with SO_2 to form gypsum. This suggests that the intimate contact between the sorbent and the coal may be the reason for the improved sorption in CWLM[3].

5.1.5 The effect of the intimate contact of coal and limestone in the agglomerate

The possibility that the improved sorbent utilization of the CWLM is due to the intimate contact of coal and limestone in the agglomerate becomes clear after proving that the limestone particles are sulfated in the agglomerate. Shorter diffusion distances and the increase in the available sorbent area provided by the fine sorbent may help to improve the sorption efficiency. To test this hypothesis, coal-limestone briquettes (CLB) were prepared using the same grind of limestone and coal used in the CWLM. The briquettes in this case simulated the char-sand agglomerates.

It was impossible to prevent breakage of some of the briquettes while they were

fed in the bed by the auger. Augered briquette particles were recovered from the auger and were double screened to obtain a particle distribution. It was estimated that 20% by weight of the fuel was entering the combustor as particles smaller than 500 microns sieve diameter (Figure 5.5). Furthermore, it was assumed that fuel particles this small exist as individual coal or sorbent particles and will not simulate CWLM agglomerate behavior and that the fraction of particles large enough to behave as agglomerated was sufficient to retain the validity of these tests.

This assumption is verified by the tests shown in Figure 5.6, which plots SO_2 removal vs. bed temperature for CWLM, coal-limestone briquettes, and dry limestone. Both the briquettes and CWLM show optimum temperatures for peak sorbent utilization that are significantly lower than for the dry limestone. This suggests that desulfurization takes place in the briquette particles, which burn at temperatures higher than the bed. The peak sulfur removal for the briquettes was found to be 70% compared to 78% for CWLM.

On the other hand, the sorbent utilization for the briquettes at $1500^{o}F$ can be approximated as the weighted average between the dry sorbent and CWLM sorbent utilizations at the same temperature (i.e., 0.8 $\times$ %retention for CWLM plus 0.2 $\times$ %retention for dry sorbent). It is hard to reach a definitive conclusion from the results of the briquette tests.

5.1.6 The effect of gasification conditions in the emulsion phase

Another explanation that may be given to the improved sorbent utilization in CWLM is the possibility of a gasification environment existing around the calcining limestone. Equilibrium calculations performed for the bubble phase in the fluidized

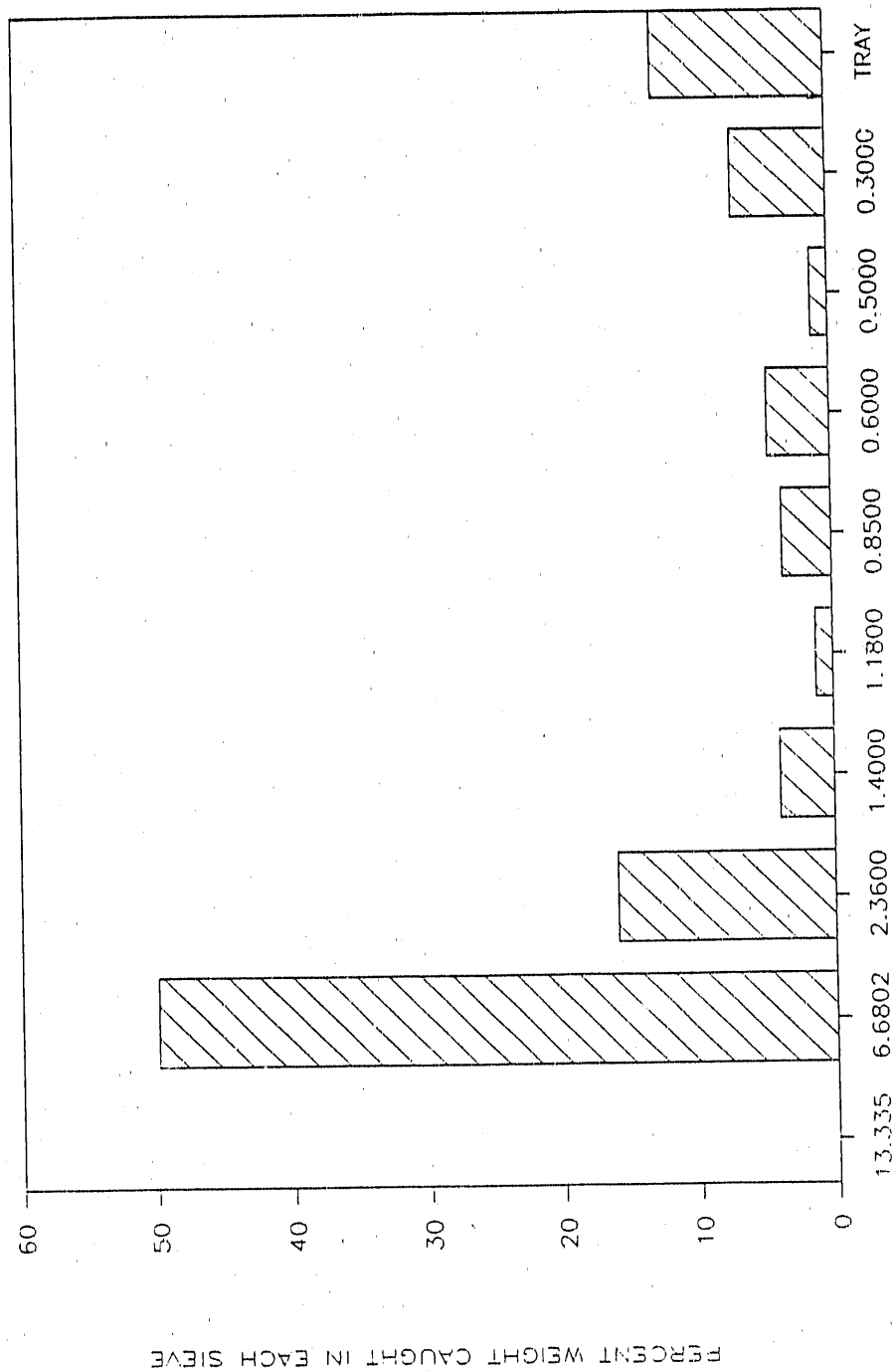

Figure 5.5: Percent weight distribution of augered briquettes

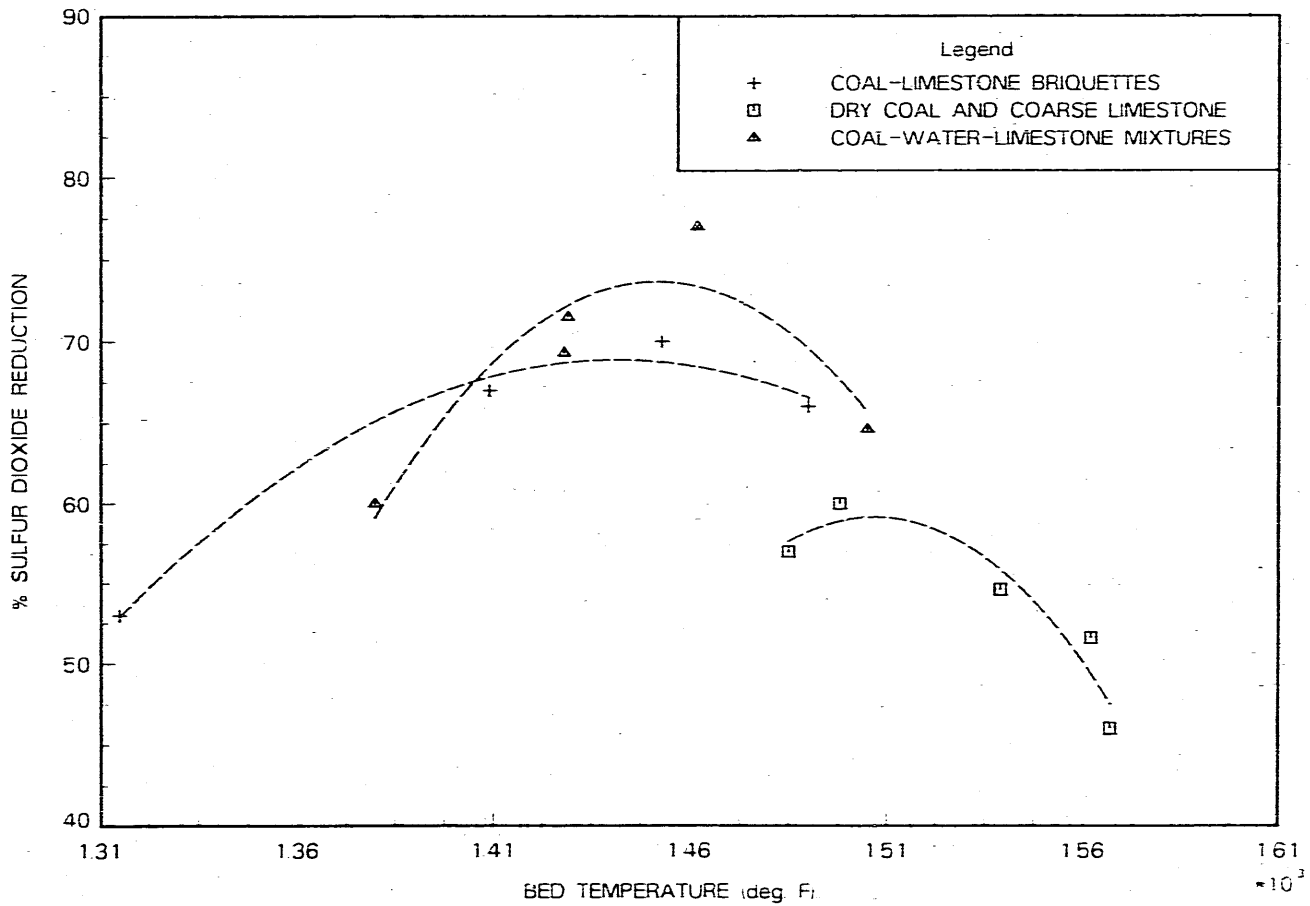

Figure 5.5: Sorbent utilization vs. bed temperature for CLB, dry limestone, and CWLM

bed do not support this notion; equilibrium calculations treat the combustor as a well stirred reactor, showing that there is enough oxygen to yield a very low partial pressure for CO. However, Ljüngstrom[24] has shown that substoichiometric conditions may exist locally in the emulsion phase. Furthermore, several models of burning coal particles suggest that CO concentrations around coal particles may be very high[25]. The high CO concentrations combined with the high water vapor content of CWLM might promote the gas-vapor reaction:

$$CO + H_2O \rightarrow CO_2 + H_2 \tag{5.2}$$

The gasification environment may thus be promoted in either the emulsion phase or the boundary layer around the agglomerate. Under gasification conditions, there is a high concentration of CO_2 that will tend to slow the calcination reaction (Equation 2.1) by shifting the equilibrium to the left. Slower calcination reduces the production of active sites on the surface of the sorbent. The rate of calcination may then be overtaken by sulfation which will, eventually, promote pore plugging. However, the high local concentrations of CO and H_2 promoted by the gasification environment may reduce $CaSO_4$ into CaO and SO_2(Equations 2.10). Accordingly, calcination may proceed to completion before sulfation began to plug the pores.

To test the hypothesis that local gasification conditions are responsible for the improved SO_2 sorption in CWLM, a water injection test was performed. The fuel used was coal-limestone briquettes. Water was injected via the CWM nozzle. A 3-scfm purge air stream was used in the nozzle to atomize the water prior to entering the combustor. The water flow-rate was adjusted so that the moisture in the bed was around 47%. The test aimed to simulate CWLM with 53% solids loading.

The gasification test was carried out at $1407^{\circ}F$ and yielded a 62% sulfur sorption.

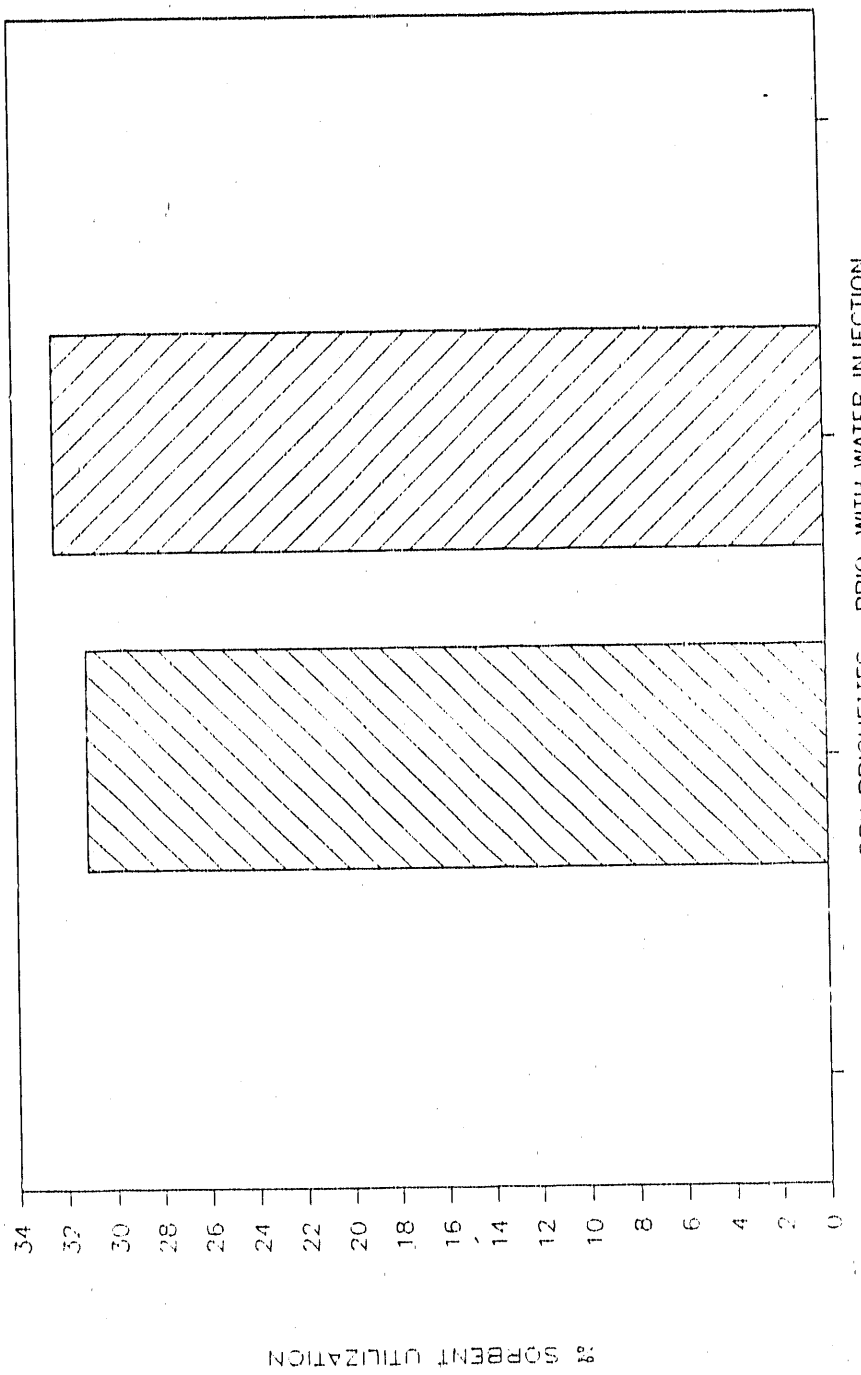

Figure 5.6: Sorbent utilization vs. bed temperature for CLB, dry limestone, and CWLM

Figure 5.7 shows the results of this test in comparison to a dry CLB at around $1390^{o}F$ which has the similar sulfur sorption as the gasification test. The water injection test proved that gasification conditions in the emulsion phase are not the reason for the improved sorbent utilization in CWLM.

5.2 In-situ Measurements of Sorbent Kinetics

5.2.1 Basic principles

Sorbent reactivity is greatly dependent on the conditions under which calcination and sulfation take place.[26] Sorbent reactivity is generally measured under well controlled conditions in a packed bed or a thermogravimetric balance[27][26]. It is possible that the local conditions of a CWLM agglomerate or a coal-limestone briquette yield different limestone reactivities than dry limestone.

The evidence presented in the previous sections proved that the mechanisms of sulfur sorption in CWLM differ significantly from dry limestone. Consequently, the kinetics of sulfur sorption in the CWLM agglomerates may be different than for the dry sorbent. It is not yet evident how the reactivity of the sorbent can be measured under these conditions.

The rate of production of volatile matter from the emulsion phase of a fluidized bed combustor may be approximated with the differential equation:

$$\frac{dC'}{dt} = -\frac{u}{L}C' + g - r \tag{5.3}$$

where C' is the volatiles concentration leaving the bed, u is the superficial velocity of the gas through the bed, L is the bed height, g is the rate of generation of volatile matter from the fuel particles, and r is the rate of removal of volatile matter due

to reaction with other bed species. Equation 5.3 can be applied for the rate of production of SO_2 from the bed. In this case, r will be the rate of sulfur sorption by limestone.

Transient operation of the combustor is required in order to estimate the rate of production of gaseous matter from the bed. The model is applicable the estimation of calcination and sulfation rates as well as in measuring burning rates of fuel.

5.2.2 Application of the model in evaluating rates of sulfur release from coal

The model introduced in the previous section will be applied to estimate the rate of generation of SO_2 from coal. The concentration C represents the concentration of SO_2 in the flue gas.

Several transient tests were carried out using 3/8-inch×8-mesh Illinois N^o5 coal. The coal was burned in a six-inch deep bed with no sorbent addition. Each test was carried at a different bed temperature, therefore a different fuel feed rate. The excess air in the bed during steady state was maintained at a nominal 20%. Once steady state was reached, the fuel was shut off and the SO_2 transient decay was recorded at 3 second intervals. The generation rate of SO_2 in the bed under transient conditions has two contributions:

$$g = g' + g'' \tag{5.4}$$

where g' is the generation rate of SO_2 associated with the volatiles release and g'' the rate of generation of SO_2 from the combustion of the devolatilized char. Volatile release from the coal is a very fast process[11]. Therefore, the time constant associated with g' must be very small. On the other hand, the generation of SO_2 associated

with the char combustion is relatively slow and steady process. The decay of SO_2 with time for one of the transient tests is shown in Figure 5.4.

The general first-order expression describing the evolution of volatile matter from coal is:

$$\frac{dN}{dt} = -k_a N \tag{5.5}$$

where k_a is the first-order rate constant for sulfur release with volatile matter[28]. Solving for N:

$$N = N_o \exp(-k_a t) \tag{5.6}$$

where N_o is the initial mass of volatile sulfur content of the coal charged in the combustor.

The number of moles of sulfur released from the coal is equal to the number of moles of SO_2 generated in the bed (assuming 100% conversion). Therefore:

$$g' = k_a N \tag{5.7}$$

Assume that the contribution of g'' is small and constant over the time period that g' is acting. Substituting Equations 5.4, 5.6, and 5.7 into Equation 5.3, and setting C equal to the concentration of SO_2 in the flue gas ($[SO_2]$) and solving for $[SO_2]$ as a function of time:

$$\begin{aligned}[SO_2] = {} & \frac{k_a N}{u/L - k_a}\left[\exp(k_a t) - \exp\left(-\frac{ut}{L}\right)\right] \\ & + \frac{g'' L}{u}\left[1 - \exp\left(-\frac{ut}{L}\right)\right] + [SO_2]_o \exp\left(-\frac{ut}{L}\right)\end{aligned} \tag{5.8}$$

where $[SO_2]_o$ is the steady state concentration of SO_2 measured at the beginning of the transient period.

Define $g''L/u$ as $[SO_2]^*$, the quasi-steady concentration of SO_2 reached when devolatilization is over (as t becomes very large). Rearranging terms and setting L/u approximately equal to 0.2 seconds (L is 1/2 foot and the superficial air velocity is on the average 2.5 ft/s), Equation 5.8 can be simplified to:

$$\ln \frac{[SO_2] - [SO_2]^*}{[SO_2]_o - [SO_2]^*} = -k_o t + \ln \frac{k_o N}{u/L - k_o} \tag{5.9}$$

The logarithm of the normalized decay of SO_2 on the left of Equation 5.9 is plotted versus time for each transient test. Linear regression of the SO_2 variable gives the characteristic time for volatile sulfur release ($\tau_c = 1/k_o$). In this case, the time t is corrected for the delay associated for the plug flow of the gas from the bed surface to the gas analyzers via the freeboard and sampling lines. The results for the characteristic times of seven transient tests are shown in Table 5.2.

Very limited work has bed done in measuring characteristic SO_2 release times during coal devolatilization. Moffat[11] observed that the sulfur release during pyrolysis of coal particles is a very fast process. Typical rates for devolatilization of small coal particles (d_p < 100 microns) can be found in Howard[29], and they are of the order of 1 second. On the other hand, the characteristic times for sulfur release in the present experiments with relatively large coal particles ($\bar{d}_p$ = 5.94 mm) were found to be of 8.4 seconds (averaged from Table 5.2).

Essenhigh[30] tested relatively large coal particles (sized 0.295-4.76 mm) which are expected to display mass-transfer-limited devolatilization, i.e., the rate of devolatilization from these particles is limited by diffusion of the volatile species through the particle pores and gas film surrounding the particle. Using a shrinking liquid sphere model for the volatiles within the coal particle, Essenhigh[30] related de-

Table 5.2: Characteristic volatile release times.

Bed Temperature (^oF)	Characteristic time (τ_c) (sec.)
1394	7.998
1464	9.442
1491	9.163
1501	8.236
1520	10.585
1553	6.494
1572	7.143

volatilization time to particle diameter as:

$$t_v = K_v d^2 \tag{5.10}$$

where d is the particle diameter and K_v is the devolatilization constant in s/mm^2. The average value of K_v for Essenhigh's[30] data is found to be $0.9s/mm^2$. Using Equation5.10 (and setting $t_v = 3 \times$ the time constant, t_c), the mean diameter of the coal charged the combustor at the beginning of the transient tests was around 5.3mm. It is still difficult to draw definitive conclusions since the coal feed for the transient tests was not monodispersive and K_v is certainly different for the coals tested by Essenhigh[30] and the Illinois N^o5 used for the transient tests. Nevertheless, this estimate of coal particle size from sulfur release rates is in reasonable agreement with the actual feed size.

5.2.3 Measuring calcination and sulfation rates using the model for sulfur release

The reaction of SO_2 with lime may be summed up as:

$$CaO + SO_2 + 1/2O_2 \rightarrow CaSO_4 \tag{5.11}$$

The sulfation rate is observed to be of first order with respect to $[SO_2]$[27] and zeroth order in oxygen concentration [31]. The reaction takes place after SO_2 is adsorbed on the lime surface:

$$a + s \rightarrow a * s \tag{5.12}$$

where a are active sites and s is the SO_2 adsorbed.

The rate of sulfation is equivalent to the rate of consumption of active sites. Assuming that the sulfation reaction is essentially irreversible, and accounting for the fact that the reaction rate does not depend on oxygen:

$$\frac{d(a * s)}{dt} = k_s C_v C_s \tag{5.13}$$

The total number of active sites may be expressed as:

$$C_{a_t} = C_v + C_{a*s} \tag{5.14}$$

Substituting in the rate equation:

$$\frac{da * s}{dt} = k_s [C_{a_t} - C_{a*s}] C_s \tag{5.15}$$

Dividing this equation with the initial number of active sites a_i and defining fractional conversion as:

$$\alpha = \frac{C_{a*s}}{a_i} \tag{5.16}$$

the pore closure model of sulfation reduces to:

$$\frac{d\alpha}{dt} = k_s C_s[\alpha_\infty - \alpha] \tag{5.17}$$

where α_∞ is the maximum fractional conversion for a particular sorbent.

This simple model can be used to describe the rates of change of $CaSO_3$, CaO, and SO_2 in the be of an FBC. The limestone rate of consumption is given by:

$$\frac{d[CaCO_3]}{dt} = f - k_c[CaCO_3] \tag{5.18}$$

where f is the feed rate of limestone in the bed and k_c is the specific rate constant for calcination. Now, the rate of consumption of the calcined limestone (lime) is:

$$\frac{d[CaO]}{dt} = k_c[CaCO_3] - k_s\alpha_\infty C_{a_t} C_s \tag{5.19}$$

Recalling Equation 5.3 and substituting for the rate of absorption of SO_2 by limestone (r):

$$\frac{dC_s}{dt} = -\frac{uC_s}{L} - k_s\alpha_\infty C_{a_t} C_s + g \tag{5.20}$$

where g is the uniform rate of generation of SO_2 within the bed. Solving for limestone concentration from Equation 5.18 as a function of time:

$$[CaCO_3] = \frac{f[1 - \exp(-k_c t)]}{k_c} \tag{5.21}$$

Finally, assume and that a quasi-equilibrium state is achieved for the rate of consumption of CaO (C_{a_t}):

$$C_{a_t} = \frac{k_c[CaCO_3]}{k_s\alpha_\infty C_s} \tag{5.22}$$

Substituting the last two equations in Equation 5.20 and rearranging:

$$\frac{dC_s}{dt} = -\frac{uC_s}{L} - f[1 - \exp(-k_c t)] + g \tag{5.23}$$

The above equation can be solved with Laplace transforms (replacing C_s with $[SO_2]$):

$$[SO_2] = \frac{f}{u/L - k_c}[\exp(-k_c t) - \exp(-\frac{ut}{L})] + \frac{g-f}{u/L}[1 - \exp(-\frac{ut}{L}) + [SO_2]_o \exp(-\frac{ut}{L}) \quad (5.24)$$

As steady state is achieved the concentration of SO_2 approaches a value $[SO_2]^*$ where:

$$[SO_2]^* = \frac{g-f}{u/L} \quad (5.25)$$

Since the residence time of the gases in the bed is significantly shorter than that of calcination or sulfation, the normalized SO_2 decay may again be approximated as:

$$\ln \frac{[SO_2] - [SO_2]^*}{[SO_2]_o - [SO_2]^*} = ln \frac{f}{(u/L)} - k_c t \quad (5.26)$$

Several transient tests were carried out by injecting limestone in the bed while burning 3/8-in×8-mesh dry coal. The data were normalized (using the SO_2 concentration ratio given above) for each test and the respective values for k_c were estimated by linear regression. The experimental and computed normalized SO_2 decay are shown in Figure 5.8. The close fit to the data provides strong support for the simple model developed. The calcination constants estimated are given in Table 5.3. The average calcination rate constant was estimated to be $0.0044 sec^{-1}$ and the apparent activation energy for calcination from these data is 47.3 $\pm$ 3.6 kcal/mol. These results are in relative agreement to activation energies obtained by Kim et al.[32] for calcination of Fedonia limestone. Their tests showed that limestone particles of size 0.2 to 1.7 mm would calcine with average activation energies of 67 kcal/mol for temperatures below 1550 ^oF. This shows that the simple transient tests may be adequate for further evaluation of sorbent kinetics in the FBC.

Table 5.3: Calcination rate constants

Bed Temperature (^oF)	Calcination rate constant (k_c) (sec^{-1})
1467	0.00804
1490	0.00292
1539	0.00382
1567	0.00273

This analytical technique may be applied to CWLM to determine intrinsic rates for calcination within the agglomerate. These will help to determine whether a unique sulfation and calcination environment, within the interior of the agglomerated fuel, is responsible for the improved sorbent utilization. Furthermore, the transient technique may be applied to monodispersive coal samples injected into an FBC operating at steady state on a baseline crushed coal. Perturbation from the steady state can provide significant information about the mechanisms of coal combustion, sulfur release rates, and calcination rates.

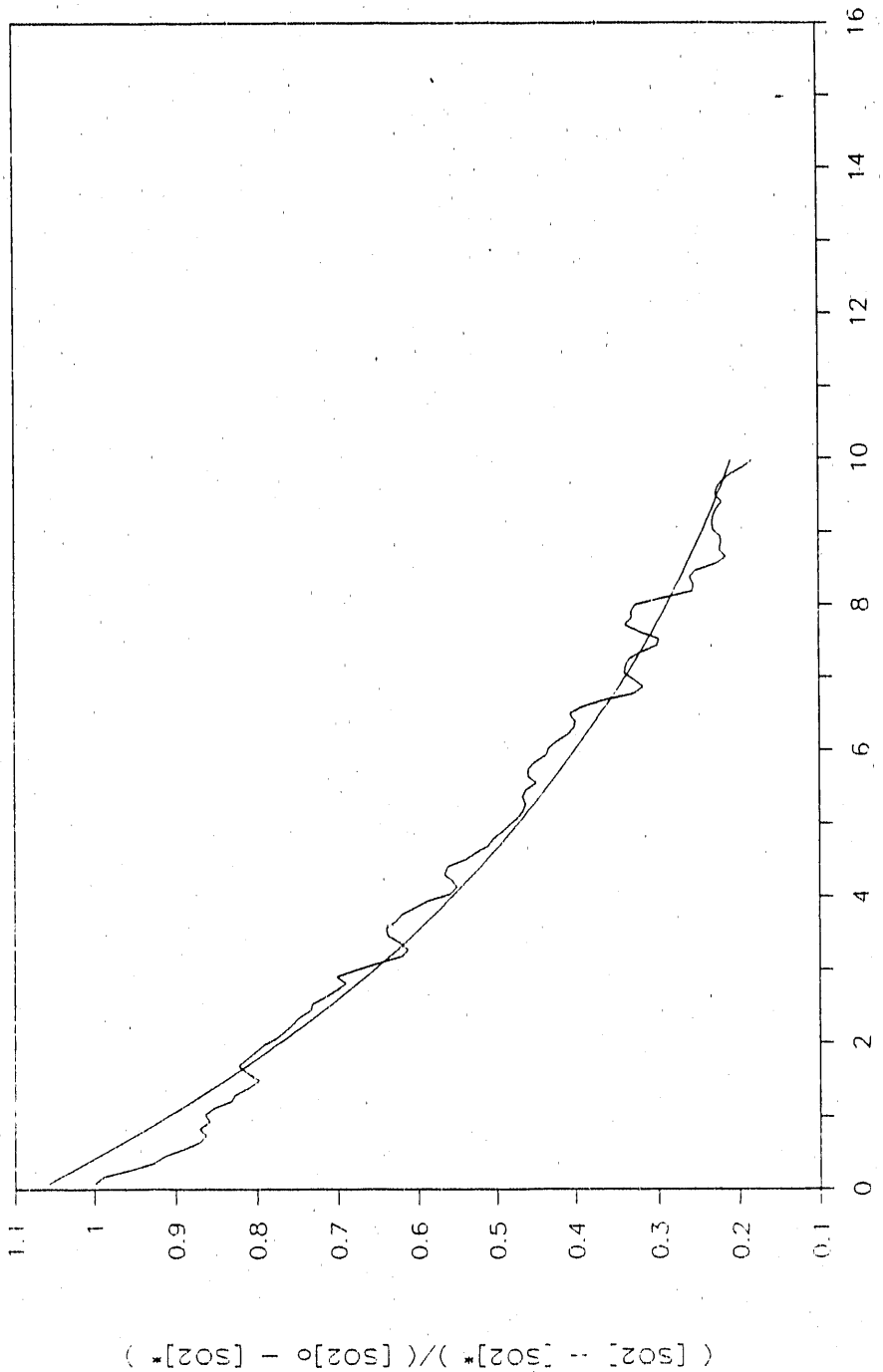

Figure 5.8: Comparison of experimental and computed normalized SO_2 decay

6. CONCLUSIONS

Sorbent utilization for dry sorbent and CWLM was found to be comparable at around 1500 ^oF, provided that a non-elutriable sorbent is used with the dry fuel. When the finer sorbent was used with dry coal, sorbent utilization was severely degraded by elutriation.

The maximum sorbent utilization for CWLM occurs 60 ^oF below the respective peak for dry sorbent, thus suggesting that both calcination and sulfation occur within the char-sand agglomerates formed when CWLM are sprayed in the bed. X-ray fluorescence scan on a sample of agglomerates showed that a large portion of the sulfur is retained in the agglomerates. This confirms that the sulfur is retained by the sorbent before the agglomerates break to release individual sorbent particles.

The peak sulfur sorption for CWLM is significantly higher than the respective peak for dry coal. The possibility of a reducing environment in the agglomerate being the reason for the higher sorbent utilization was examined by recovering samples from the bed after a quench test. XRD analysis of agglomerated material from the bed showed no traces of CaS which is the expected product of reducing conditions. Conditions inside the agglomerate may be described as oxidizing rather than reducing.

Dry briquette tests showed a slightly different sorption mechanism compared to CWLM. This was partly attributed to the breakage of briquette particles while

feeding them in the bed. However the optimum temperature for sulfur sorption when burning briquettes was found to be significantly lower than for dry sorbent. This shows that there are enough sizable particles left, while feeding briquettes, to simulate agglomerate behavior. The sorption mechanism for briquettes may be a combination of CWLM simulated by the 80% coarse particles and the 20% fines produced. The fines will behave as individual coal and sorbent particles fed in the bed.

Gasification in the bubble phase was excluded since there is an abundance of oxygen in the bed. Furthermore, gasification in the emulsion phase was examined by injecting water in the bed during the combustion of briquettes. The water injection test showed no significant change in sorbent utilization compared to dry briquettes.

The peak sorbent utilization for CWLM is higher than for the dry sorbent and occurs at lower temperatures. The improved sorbent utilization is most possibly due to the intimate contact of coal and limestone in the CWLM agglomerate.

Finally, transient operation of the combustor was found to be extremely useful in determining characteristic volatile release times and intrinsic reaction rates for calcination. Several transient tests with dry coal in the absence of sorbent showed characteristic volatile release times to be on the order of 8 seconds. Sorbent transient tests revealed calcination rate constants of $0.0044 sec^{-1}$ and an activation energy of 47.3 ± 3kcal/kmol-K.

Future work may involve the applicability of this technique in determining rates of sulfation and calcination in CWLM agglomerates and sulfur release rates during steady state operation of the combustor.

7. BIBLIOGRAPHY

[1] A. Roberts, K. Pillai, and L. Carpenter. *Combustion of "run-of-mine" coal and coal-water mixtures in a small PFBC.* Proc.-7th International Conference on Fluidized Bed Combustion, Philadelphia, Pa., 1982, pp. 482-489.

[2] U. Arena, G. De Michele, L. Massimilla, and M. Miccio. *Coal water slurry utilization in fluidized bed combustion.* Proc.-6th International Symposium on Coal Slurry Utilization in Fluidized Bed Combustion, Orlando, Fla., 1984.

[3] K. Cen, X. Cao, Z. Yuan, S. Kong, J. Hong, M. Xie, D. Lu, M. Ni, Y. Chen. *Combustion and gasification of coal-water slurry in fluidized beds.* Proc.-7th International Conference on Fluidized Bed Combustion, Philadelphia, Pa., 1982, pp. 253-263.

[4] J. S. Mei, J. C. Cho, and D. Martin. *Microstructural characteristics of char-agglomerates.* Sixth International Conference on Coal-Liquid and Alternative fuels, Halifax, Nova Scotia, 1986.

[5] R. C. Brown, W. H Buttermore, and J. E Foley. *The evaluation of midwestern coal and limestone in coal-liquid fuels for fluidized bed combustors.* Proc.-10th International Conference on Slurry Technology, New Orleans, La., 1987, pp. 49-56.

[6] J. Gregory and R. C. Brown. *Combustion behavior of coal-water mixtures in fluidized beds.* Proc.-10th International Conference on Fluidized Bed Combustion, San Francisco, Ca., 1989, pp.77-84.

[7] R. C. Brown and Nearchos Christofides. *Attrition and fragmentation of coal-water mixtures in fluidized beds.* Proc.-3rd International Conference on Processing and Utilization of High Sulfur Coals, Ames, Ia., November 14-16, 1989.

[8] G. De Michelle, M. Graziadio, and S. Pasini. *Combustion tests of coal-water slurry on industrial boilers.* Combustion of Tomorrow's Fuels: Selected papers

from conferences held in Santa Barbara, California, November 1982, and Davos, Switzerland, October 1984, New York, NY, 1988, pp. 731-745.

[9] A. R. Kernstein and S. Niksa. *Fragmentation during carbon conversions: Predictions and measurements.* 20th International Symposium on Combustion, The Combustion Institute, Pittsburgh, Pa., 1984, pp. 941-949.

[10] Reviews in Coal Science, IEA Coal Research. Butterworths, London, 1989.

[11] A. J. Moffat. *The chemistry and mechanism of sulfur release in during coal combustion.* Proceedings of the Central States Section of the Combustion Institute, March 22-23, 1982

[12] D. Schmal. *Improving the action of sulfur sorbents in the fluidized-bed combustion of coal.* Industrial Engineering Chemical Process Des. Dev., 24 (1985): 72-77.

[13] J. G. Yates. Fundamentals of Fluidized-Bed Chemical Processes. Butterworths, London, 1983.

[14] A. A. Jonke, G. J. Vogel, E. L. Carls, D. Ramaswami, L. Anastasia, R. Jarry, and M. Haas. *Pollution control capabilities of fluidized-bed combustors.* Air Pollution and its Control, A.I.Ch.E. Symposium Series, R. W Coughlin, A. F. Sarofim, N. J. Weinstein, Vol. 68, No. 126, New York, New York, 1972, pp. 241-251.

[15] S. C. Saxena. *Mathematical models for fluidized-bed coal combustion and sulfur retention.* Energy(Oxford), 13, No. 7 (1988): 557-607.

[16] G. A. Simons, A. R. Garman, A. A. Boni. *The kinetic rate of SO_2 sorption by CaO.* A.I.Ch.E. Journal, 33, No. 2 (February 1987): 211-217.

[17] B. Bonn and H. Münzner. *Sulphur capture with limestones in fluidized bed combustion.* Fluidized Bed Combustion: Systems and Applications. Institute of Energy, London, England, 1980, pp. v-3-1 to v-3-7.

[18] L. Green, Jr. *Utilization of medium-sulfur slurry fuels by a fluid-bed calcium/sulfur contactor.* Proc.-2nd Annual Pittsburgh Coal Conference, Pittsburgh, Pa., September 16-20, 1985, pp. 112-119.

[19] P. Basu. *Burning rate of carbon in fluidized beds.* Fuel, 56 (1977): 390-392.

[20] G. S. Trivett, R. Z. Soloma, R. S. Field, A. M. Al Tower, and G. D. M. McCay. *Improved operation of an atmospheric pressure fluidized bed using coal-water mixtures.* European Conference on Coal Liquid Mixtures, London, England, 1985, pp. 147-162.

[21] J. E. Foley, R. C. Brown, and W. H. Buttermore. *Heat transfer in a two bed fluidized bed combustor.* Proceedings 26th National Heat Transfer Conference, Philadelphia, Pa., August 6-9, 1989.

[22] J. E. Stantan. *Sulphur retention in fluidized bed combustion.* Fluidized Beds: Combustion and Applications. J. R. Howard. Applied Science Publishers, Essex, England, 1983, pp. 199-226.

[23] B. J. Zobeck, M. D. Mann, T. A. Potas, and D. J. Maas. *Firing low-rank coal-water fuel in a fluidized bed combustor.* 14th Biennial Lignite Symposium, Dallas, Tx., May 18-21, 1987.

[24] E. B. Ljüngstrom. *In-bed oxygen measurements in a commercial-size AFBC.* Proceedings 8th International Conference on FBC, Houston, Tx, 1985, pp. 853-864.

[25] R. H. Essenhigh. *Fundamentals of coal combustion.* Chemistry of Coal Utilization, M. A. Elliot. Wiley, New York, 1981, pp. 1153-1312.

[26] D. L. Keairns, G. C. Williams, C. Georgakis, J. Chrotowski, R. Newby, and N. H. Ulerich. *Sulfur emissions control in atmospheric fluidized bed combustion.* DOE Technical Report, DOE/MC/14536-2544, January 1987, pp. 7-49.

[27] T. Mulligan, M. Pomeroy, and J. E. Bannard. *The mechanism of the sulphation of limestone by sulphur dioxide in the presence of oxygen.* Journal of the Institute of Energy, 62 (May 1989): pp. 40-47.

[28] M. Saito, M. Sadakata, M. Sato, and T. Sakai. *Devolatilization characteristics of single coal particles for combustion in air and pyrolysis in nitrogen.* Fuel, 66 (May 1987): 717-721.

[29] J. B. Howard. *Fundamentals of coal pyrolysis.* Chemistry of Coal Utilization: Second Supplementary Volume, M. A. Elliott Ed, Wiley, New York, NY, 1981.

[30] R. H. Essenhigh. *The influence of coal rank on the burning times of single captive particles.* J. Eng. Power, 85 (1963): 183.

[31] G. A. Simmons, T. E. Parker, and J. R. Morency. *The oxygen reaction order of SO_2 with CaO.* Combustion and Flame, 74 (1988): 107-110.

[32] H. T. Kim, J. M. Stencel, and J. R. Byrd. *Limestone calcination and sulfation microstructure, porosity and kinetics under AFBC environments.* Proceedings of the 8th International Conference on Fluidized Bed Combustion, Boston, Massachusetts, 1987, pp. 449-457.

[33] R. H. Petrucci, General Chemistry:Principles and Modern Applications, 2nd ed. Macmillan, New York, c1977, p. 268.

8. APPENDIX. ESTIMATING THE ACID CONCENTRATION OF THE CONDENSATE

It has been previously mentioned that condensation of acid mist or water vapor in the gas sampling lines may result in scrambling of the SO_2 readings and may even damage the gas analyzer cells. Thus an impingment filter was installed down stream of the Perma-Pure dryer to avoid such a condensate to reach the instruments. Additionally, the condensate could be collected and checked for acidity.

One such sample was collected after a 2 hour CWLM test. The analysis that follows estimates the precise amount of SO_2 dissolved in the condensate.

The amount of condensate involved was around 3.2 ml and had an approximate pH of 2. The pH of a solution is defined as the negative logarithm base 10 of the concentration of hydrogen ions (H^+) [33]:

$$pH = -\log_{10}[H^+] \tag{8.1}$$

When SO_2 is dissolved in water, the following reactions take place:

$$SO_2 + O_2 \rightleftharpoons SO_3 \tag{8.2}$$

$$SO_3 + H_2O \rightleftharpoons H_2SO_4 \tag{8.3}$$

The sulfuric acid produced will dissociate according to the reactions:

$$H_2SO_4 \rightleftharpoons H^+ + HSO_4^- \tag{8.4}$$

$$HSO_4 \rightleftharpoons H^+ + SO_4^- \tag{8.5}$$

The equilibrium constant for the first reaction is $k_a1 = 10^3$ and for the second reaction $k_a2 = 0.012$. The total equilibrium constant for the solution is estimated to be:

$$K_a = \frac{[H^+]^2[SO_4]^=}{[H_2SO_4} = k_{a1} \times k_{a2} = 12 \tag{8.6}$$

Now, from the pH value:

$$pH = 2.0$$

$$\Rightarrow [H^+] = 0.01 \text{ mole/lt}$$

The amount of sulfuric acid is calculated from the equilibrium constant since $[SO_4^=]$ is equal to $[H^+]/2$. Thus the concentration of H_2SO_4 is found to be:

$$[H_2SO_4] = \frac{[H^+]^2}{2K_a} = 4.16 \times 10^{-8} mole/lt \tag{8.7}$$

From Equation 8.2, it is estimated that 1 mole of SO_2 will produce 1 mole of H_2SO_4. Thus, 4.16×10^{-8} moles/lt of sulfur dioxide are dissolved (assuming that the contribution of the reverse reactions in Equation 8.2 are negligible). Since 3.2 ml of solution were obtained, the amount of SO_2 removed from the gas stream, during the test, is 1.33×10^{-10} mole/lt.

The total number of moles of SO_2 produced when no limestone is added may be found from the ideal gas law,

$$n = \frac{P}{RT} \times Q \tag{8.8}$$

where Q is the available gas flow. The total flow-rate of the sample is 7 scfh. Thus, the total flow-rate of is 0.01787 moles/hour. When no sorbent is added in the bed, the SO_2 concentration is approximately 2120 ppm or 0.00212 %. Thus the total amount of SO_2 produced is:

$$SO_2 \text{ in flue gas} = 0.002120 \times 0.01787 = 3.79 \times 10^{-5} \text{ moles/hour}$$

The amount of gas passed through the SO_2 gas analyzer is only 2 scfm, therefore only 2/7 of the amount estimated above:

$$SO_2 \text{ through gas analyzer} = 1.08 \times 10^{-5} \text{ moles/hour}$$

For a two hour test a total of 2.16×10^{-5} moles of SO_2 are passed through the analyzer. Thus the overall error may be estimated to be:

$$perc.error = \frac{SO_2 - in - condensate}{SO_2 - in - gas - stream} \times 100 = 0.0006 \tag{8.9}$$

The above error may be increased to 0.002 % if limestone is incorporated in the CWLM. The limestone may reduce the SO_2 concentration in the flue gas to 600 ppm.

From the calculations, it is obvious that the error in the reading is negligible. Despite this, the acid mist must be removed because it may damage the reading cells in the gas analyzers.

- END -

DATE FILMED

10 / 23 / 90